Metals and Materials International (2020) 26:933–960
https://doi.org/10.1007/s12540-019-00491-0

Review on the Influence of Different Reinforcements on the Microstructure and Wear Behavior of Functionally Graded Aluminum Matrix Composites by Centrifugal Casting

Bassiouny Saleh[1,2] · Jinghua Jiang[1] · Aibin Ma[1,3] · Dan Song[1] · Donghui Yang[1] · Qiong Xu[1,3]

Received: 3 May 2019 / Accepted: 1 October 2019 / Published online: 19 October 2019

Abstract
The main objective of the present paper is to draw the attention of researchers towards the wear analysis of functionally graded aluminum matrix composites (FGAMCs) reinforced with different types of particles. The quality of the products and characteristics achieved by the functionally graded materials (FGMs) has been given increasing attention during recent decades. FGMs provide a way to obtain gradients between two phases with variations of properties. The centrifuge casting process was used to produce continuous variation of graded materials. These continuous graded materials offer high strength and enhanced wear resistances compared with traditional composite materials. This paper summarizes the effect of the various reinforcement materials and wear test parameters on microstructure as well as wear properties in the FGAMCs obtained through the centrifugal casting technique. The results found in the reviewed literature are classified according to types of reinforcement particles (such as silicon carbide, alumina and boron carbide) and the influence of wear test parameters (such as applied load, sliding distance, duration and sliding speed) on FGM composites. The main conclusions in this paper are derived from previous studies on experimental investigations on the wear characteristics of FGAMCs. The research gaps and future directions have been discussed which will be prolific to the researchers in the design and manufacture of FGMs production by centrifugal casting.

Keywords Metal matrix composites (MMCs) · Functionally graded materials (FGMs) · Centrifugal casting · Sliding wear · Aluminium alloy · Ceramic reinforcement

1 Introduction

Metal matrix composites (MMCs) characterize a wide range of temperatures by very good mechanical and physical characteristics. In the last two decades, MMCs have become materials of broad technological and commercial significance, from a scientific and intellectual concern [1]. The high stiffness and weight strength, good heat resistance, excellent tribological characteristics and great fatigue characteristics are the main advantages of Aluminum MMCs [2]. These are reinforced by hard ceramic particles, such as SiC, TiC, Al_2O_3 and B_4C. Aluminum MMCs are breakable when the ceramic enhancement content is high [3]. When the weight of the reinforcement particles in the matrix material increases, aluminum MMCs become brittle [4]. This greatly reduces the area of aluminum MMCs in wear and corrosion applications [5].

Functionally graded materials (FGMs) have recently become significant to enhance the mechanical and tribological characteristics of MMCs by producing gradient transition zone between matrix and particle phases [6–10]. The concept of FGMs was first taken into consideration in Japan during a space plane project in 1984 [11], where a combination of the materials used was intended to provide a thermal barrier to resist surface temperatures of 1700 °C and 700 °C across a 10 mm thick as shown in Fig. 1 [12, 13]. Then over the past thirty years FGMs have been evolving significantly,

✉ Bassiouny Saleh
bassiouny.saleh@hhu.edu.cn

✉ Jinghua Jiang
jinghua-jiang@hhu.edu.cn

[1] College of Mechanics and Materials, Hohai University, Nanjing 211100, China

[2] Production Engineering Department, Alexandria University, Alexandria 21544, Egypt

[3] Suqian Institute, Hohai University, Suqian 223800, China

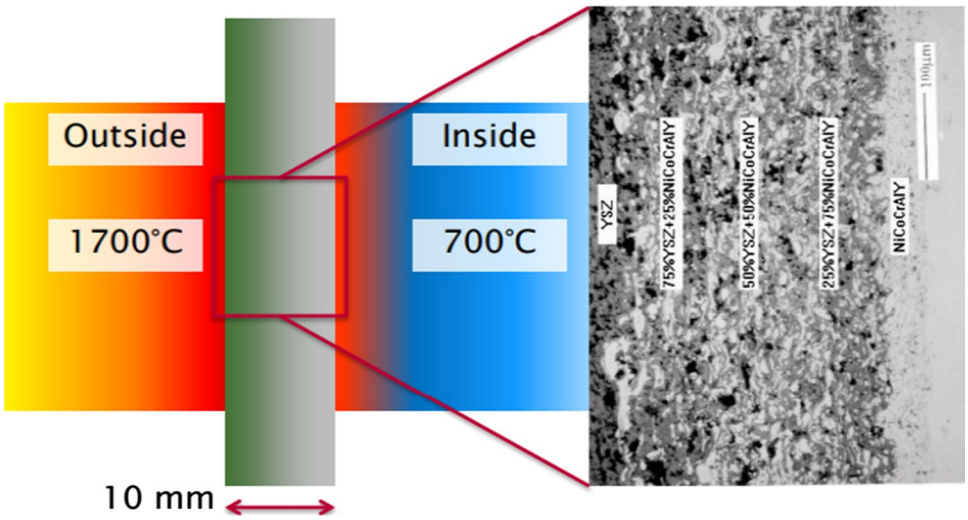

Fig. 1 First example for metallic FGM in Japan [12]

as shown in Fig. 2. Nature is the best manufacturer of FGMs and provides examples. Our nature is surrounded by examples for FGM, not new to us. The bone, the skin and the bamboo tree, for example, are all various types of FGMs [14–16]. There are various types of manufacturing methods for producing FGMs [17–20], there exist a number of well-known techniques including powder metallurgy [21–27], centrifugal casting [28, 29] or centrifugal slurry [30], vapour deposition [31–33], solid freeform (SFF) fabrication including additive manufacturing [34–37]. FGMs can be split into two broad groups as shown in Fig. 3, namely continuous grouping (such as centrifugal casting and diffusion bonding) [38, 39] and discreet grouping [40] (such as powder metallurgy and additive manufacturing) [41–48]. In continuous FGM, there is continuous gradient present from one material to the other material. This gradient happens continually with position in structure and microstructure. However, in case of discreet FGM, material gradient is provided in layered fashion [49]. This means that the microstructure feature changes in a step by step way, resulting in multilayered interface composition between discontinuous layers [44].

Specifically, the techniques of Centrifugal casting and powder metallurgy have proven effective in producing FGMs materials with gradient in microstructures and/or compositions [50, 51]. FGMs are generally more attractive to process by centrifugal casting because it produces samples which are significantly larger than those obtained with powder metallurgy [30, 52, 53]. Moreover, centrifugal casting with several advantages such as continuous distribution of particles within matrix is the most easy and cost-efficient way of making the FGMs technique compared to other methods [54–56]. Therefore, functionally graded aluminum matrix composites (FGAMCs) have been used in aerospace, automotive and other transport vehicles successfully [57], and further use with the development of centrifugal casting methods will be expected [22, 58].

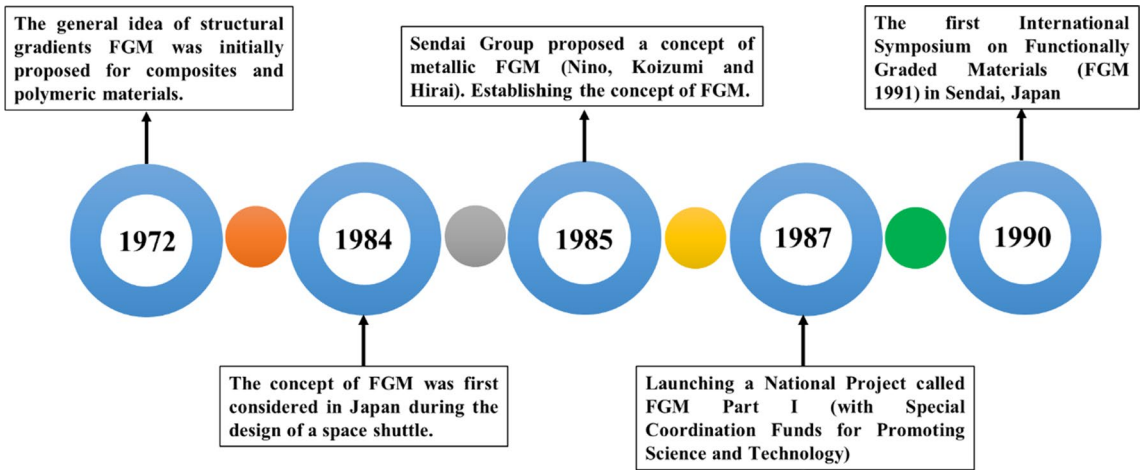

Fig. 2 Historical development for FGM [12]

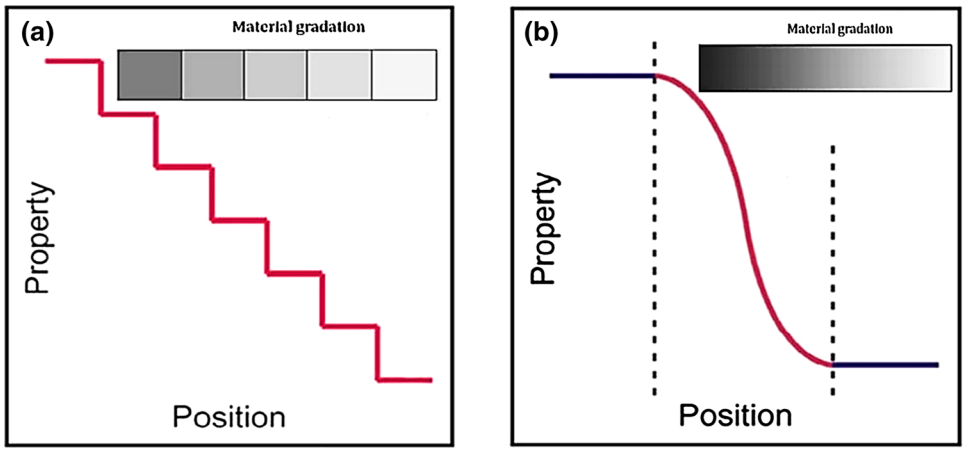

Fig. 3 **a** Discreet and **b** continuous type FGM [34]

As a substitute material, FGMs have a strong potential where conditions of operation are severe [59, 60]. Examples include flywheels [61], artificial bones [62, 63], turbine blades, heat exchanger tubes and heat-engine components [64, 65]. Coatings are generally only a layer sprayed across the substrate [66, 67].

In recent years, many researchers have carried out review papers on functionally graded materials focusing on mathematical modeling and particle simulation [68–75], while others have focused on manufacturing methods [41, 57] and applications of functionally graded materials [55, 76].

Based on the stated potential applications and benefits of FGMs, this review paper discusses the effect of reinforcement types and wear test parameters on the microstructure as well as wear behaviour of the FGM composites obtained through the centrifugal casting method. some research is presented out on FGMs, which identify the best parameters to improve wear resistance through these research work.

The rest of the paper is organized as follows: effect of reinforcement types is presented in part 2, Part 3 gives effect of wear test parameters. Recent research gaps and future directions for FGMs are presented in part 4, while summary and concluding remarks are presented in part 5. The findings described in tables of this research will be used to show improvements in mechanical characteristics and wear resistance.

2 Types of Reinforcement

Aluminum (Al), copper (Cu) and magnesium (Mg) are the most commonly used as a matrix material for producing FGMs manufactured by centrifugal casting as shown in Fig. 4. This review article focuses on aluminum alloys according to Fig. 4 in conjunction with the significant characteristics and applications of aluminum alloys. Aluminum has less weight, high thermal and electrical conductivity and is known as an attractive metal. The FGAMCs are designed

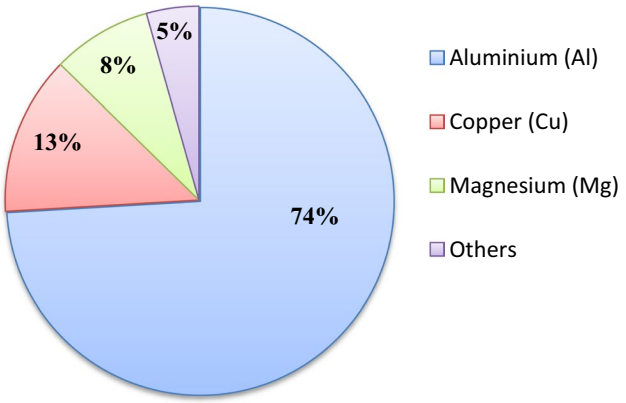

Fig. 4 Percentage of matrix type used in research papers to produce FGMs prepared by centrifugal casting (based on data from Scopus in the duration of 2000–7/2019)

for improved mechanical properties, high corrosion resistance and wear resistance [77].

In the properties of FGMs, types of ceramic particles play a crucial role. The Aluminum Alloys were currently used to develop FGMs as matrix materials and particles such as Al_2O_3, SiC, TiC,B_4C, WC, ZrO_2, TiO_2, ZrO_2, Al_3Zr, Al_3Ti, and Si_3N_4 used as reinforcements [78, 79]. In the given working temperature, the ceramic particles should be unreactive and stable. SiC and Al_2O_3 are the most commonly used reinforcements to produce FGAMCs [80, 81]. Until recently, SiC, Al_2O_3 and TiC particles reinforced materials in different types of aluminum alloys were used in several studies with FGAMCs obtained by centrifugal casting process [82].

Based on the published articles studied, the discussion on the types of particles reinforcement used in the synthesis of FGAMCs through centrifugal casting can be divided into two broad groups.

The first group is the most widely used in the manufacture of FGAMCs due to its many applications and has already

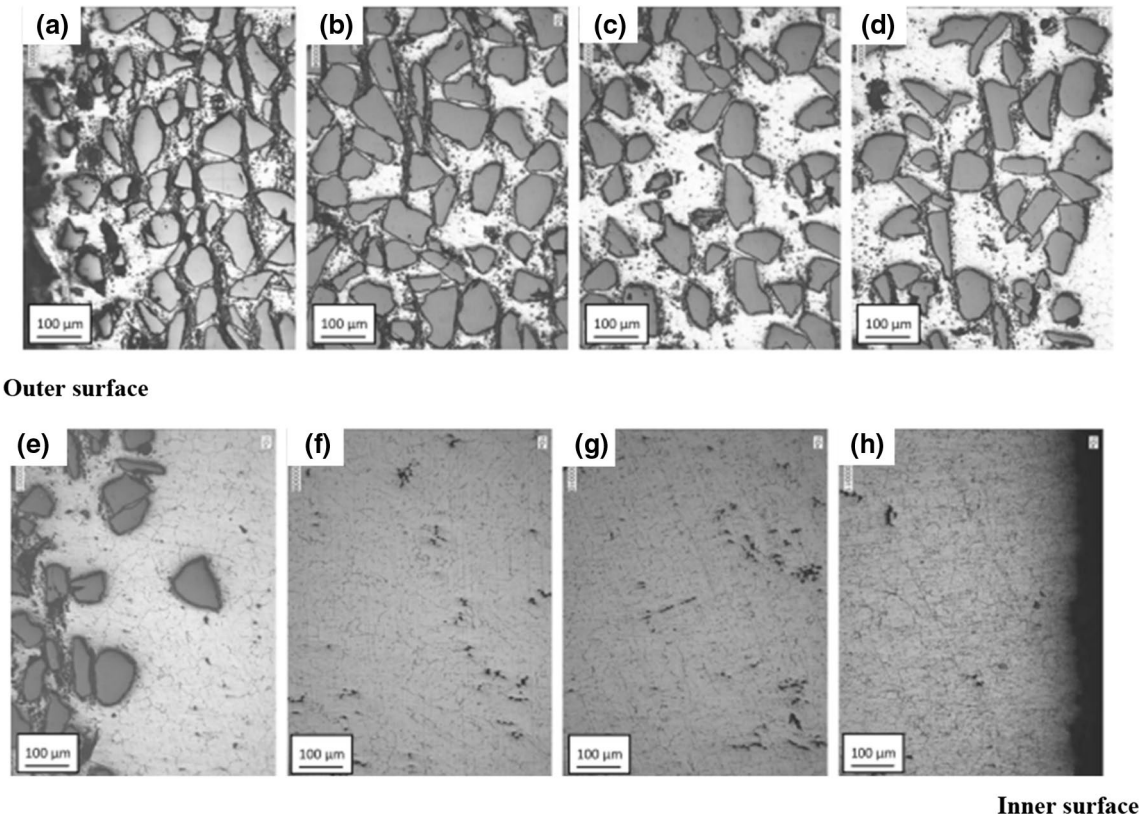

Fig. 5 Microstructures of the FG Al6061 alloy/SiC_p across the thickness from outer to inner zone [87]. **a** 1 mm, **b** 3 mm, **c** 4 mm, **d** 4.5 mm, **e** 5 mm, **f** 6 mm, **g** 8 mm and **h** 10 mm from outer surface

been studied adequately and it consists of SiC, Al_2O_3, TiC, B_4C and ZrO_2 particles. While, the second group is the least used in the manufacture of FGAMCs due to the lack of applications or difficulty in using them to obtain these gradient materials with the required characteristics and this group needs further study, which consists of WC, TiS_2, Si_3N_4 and AlB_2.

The literature review states that the microstructure and wear resistance of FGAMCs obtained through centrifugal casting are affected by types of reinforcement materials, and thus some types of particles used to manufacture these materials are summarized in the following sub-sections.

2.1 Silicon Carbide Reinforced FGAMCs

Nowadays, SiC particles in micron sizes have been used widely in FGMs to enhance the mechanical properties and improve the wear resistance of Al alloys, due to their chemical compatibility with the Al matrices [83, 84]. The factors affecting the impact behaviour of SiC particles reinforced FGAMCs are particle agglomeration, particle cracking, poor wettability and weak matrix-reinforcement bonding. The applications of FGAMCs reinforced by SiC_p produced by centrifugal casting can be found in flywheels, engine cylinder liners, pistons, connecting rod, bearings, brake drum, diving cylinders and many other fields because of all previous applications need gradient in strength, thermal, pressure and/or wear [85, 86].

Rajan et al. [87] studied the microstructure and mechanical behaviour of FG Al 6061 alloy reinforced with 20 wt% of SiC particles fabricated through horizontal centrifugal casting. The mechanical properties of the FG Al 6061–20 wt% SiC_p composites were higher than that of the base alloy. The microstructure results showed a higher concentration of particles in the outer zone of all FG Al 6061–20 wt% SiCp composites than in other zones as shown in Fig. 5.

Wang et al. [88] investigated the influence of high reinforcement concentration of FG Al–Si alloy/20 wt% SiC_P fabricated through horizontal centrifugal casting to study the microstructure behaviour and particle size distribution at different parameter. Three particle sizes are used, each with an average size of 15, 30 and 59 µm, and a weight ratio of 1:2:3, respectively. The results show that 55% of particle concentration appear in the outer zone and thus the properties in that zone are improved. The results also showed the presence of some clusters of particles in some microstructure images.

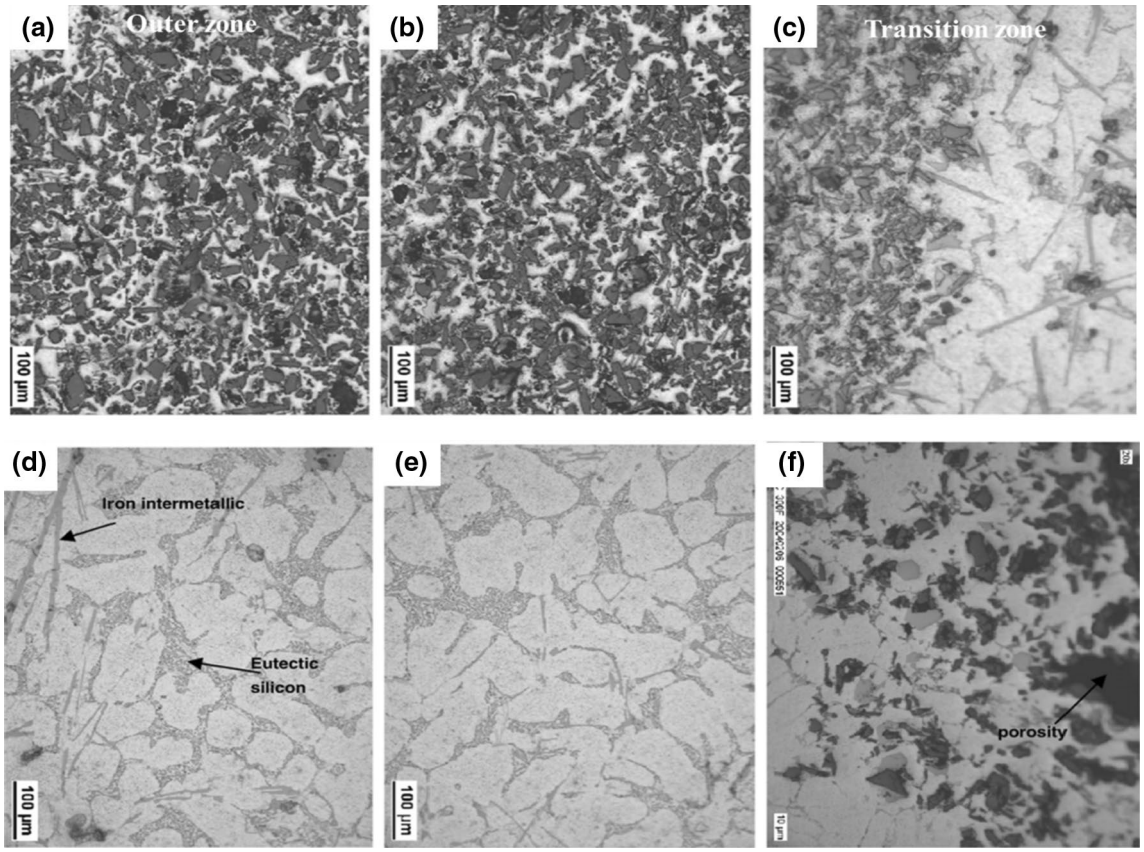

Fig. 6 Microstructures of the FG Al356 alloy/SiC_p through the thickness from outer to inner zone. **a** 1.5 mm, **b** 3.5 mm, **c** 5.5 mm, **d** 6.5 mm, **e** 12 mm and **f** 15 mm [89]

Rajan et al. [89] investigated the influence of matrix type of FG Al alloy reinforced with 15 wt% of SiC_P with 23 µm particle size fabricated obtained through horizontal centrifugal casting to study the microstructure characteristic and particle concentration. The two matrix alloys used to synthesize FGMMC are cast aluminum A356, and wrought aluminum 2124 alloys. They found that SiC particles concentrations in A356 alloy are higher than in 2124 alloy in the outer zone as shown in Figs. 6 and 7. Also, when the mould speed and pouring temperature increase, the thickness of the particles enriched area reduces.

Vieira et al. [90] investigated the wear behaviour of FG Al alloy reinforced with 10 wt% of beta SiC particles at two different mould rotational speeds using the centrifugal casting technique. The results of microstructure revealed that the outer zone of all FGAMCs exhibit higher concentration of particles than other zones as shown in Fig. 8. As beta SiC particles concentration and mould speed increase, the material weight loss is particularly reduced in the outer zone.

Babu et al. [91] studied the changes in wear rate with variation of sliding speed and applied load at different three zones of FG A356 reinforced with 20 wt% SiC particles prepared via the centrifugal casting process. They also studied the microstructure behaviour along with mechanical properties. According to the microstructure results as shown in Fig. 9, the centrifugal force led to the movement of the SiC particles to the outer zone of the FG disc, thus improving wear resistance. By analysis the variance (ANOVA), they examined wear test parameters to identify the major parameters affecting wear loss. As the contact pressure (applied load) increased from 20 to 40 N, the morphology of the worn surface gradually changed from the small grooves to large grooves and cracks.

Rodríguez-Castro et al. [92] experimented on FG A359 alloy reinforced with 20 up to 40 wt% SiC particles fabricated using centrifugal casting route at 700 and 1300 rpm. The studies highlighted the microstructural and the mechanical characteristics of FG samples. The concentration of SiC particles is increased, especially at the outer zone as shown in Fig. 10 when the weight fraction increases. The mechanical results reveal the effect on the enhancement of matrix material was limited to a certain weight fraction (30 wt%) of SiC particle reinforcement.

Jayakumar et al. [93] developed the FG AA 6061 alloy reinforced with 10 wt% of green SiC particles of 23 µm average size using centrifugal casting method to study the

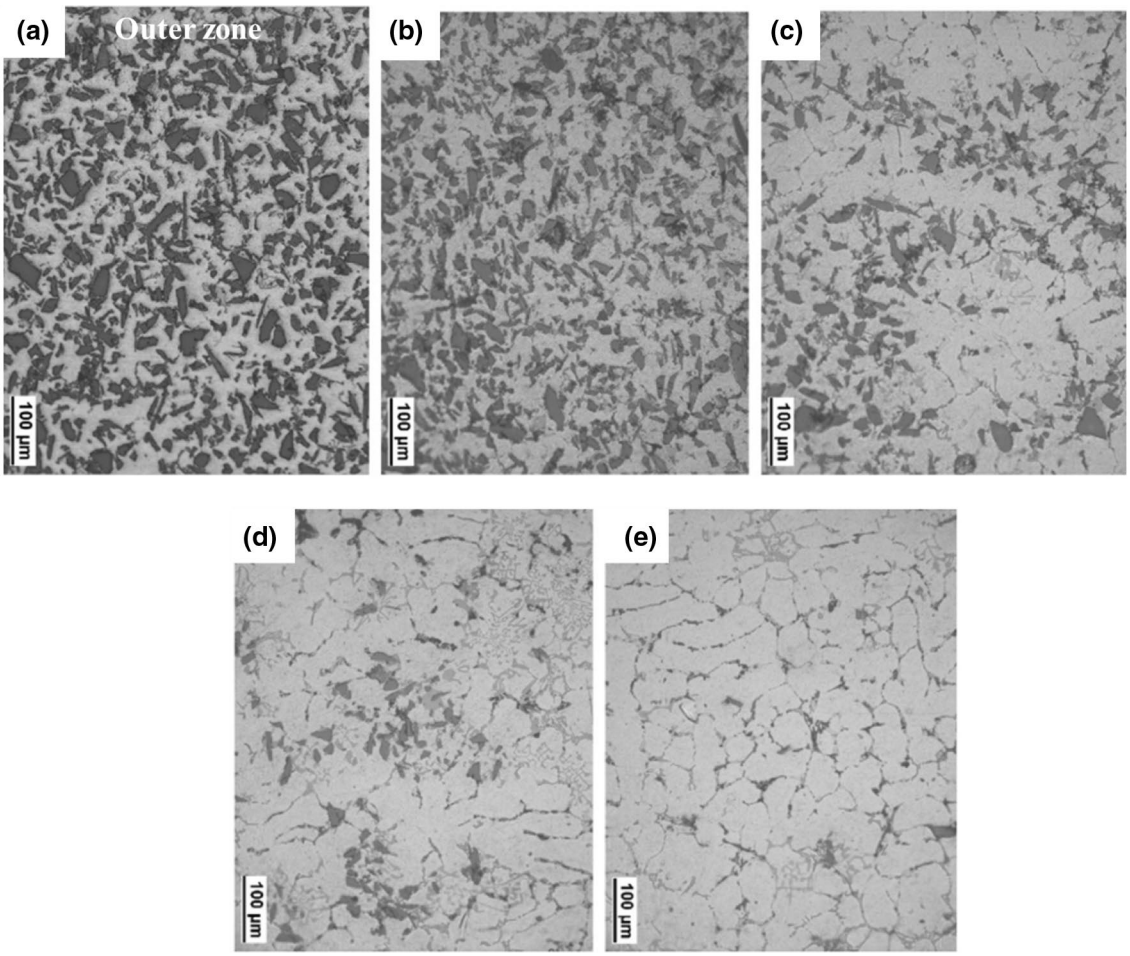

Fig. 7 Microstructures of Al(2124)-SiC FGMCC hollow cylinder at different positions from outer zone. **a** 1 mm; **b** 1.5 mm; **c** 2.5 mm; **d** 5 mm; **e** 12.5 mm [89]

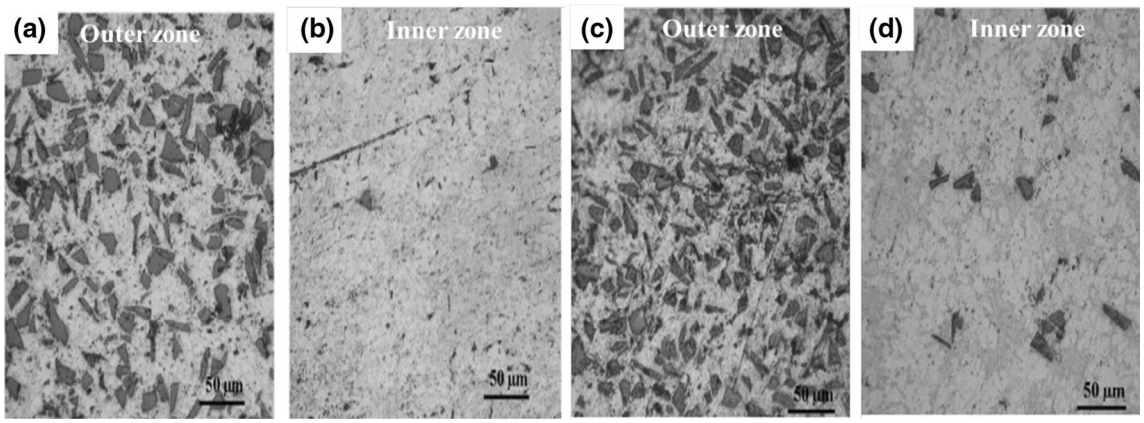

Fig. 8 Microstructures of the FG Al alloy/SiC_p at two different zones. **a** Inner zone, **b** outer zone at 1500 rpm and **c** inner zone, **d** outer zone at 2000 rpm [90]

mechanical and wear behaviour at different process conditions. Microstructure results show that the outer zone of FG rings is more concentration of particles than transition and inner zones due to centrifugal force. Therefore, the outer zone is more suitable for wear applications especially in the automotive industry.

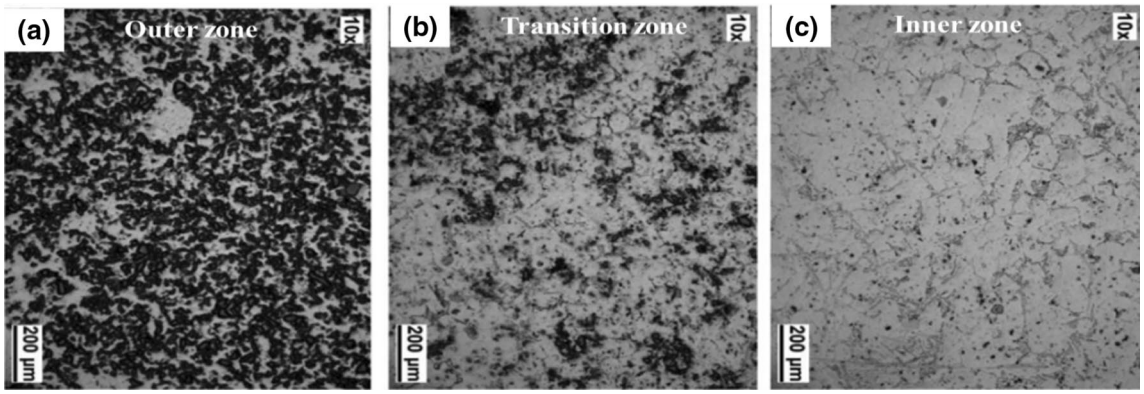

Fig. 9 Microstructures of the FG Al356 alloy/SiC_p at various distances from outer zone. **a** 15 mm, **b** 45 mm and **c** 75 mm [91]

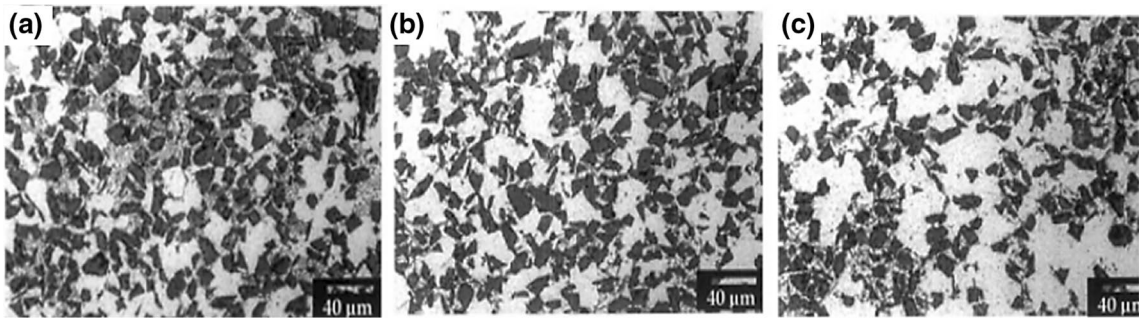

Fig. 10 Microstructures of FG Al 359 alloy/SiC_p with different locations form outer zone produced at 1300 rpm. **a** 0.79 mm, **b** 10.32 mm and **c** 26.19 mm from outer surface [92]

Savaş et al. [94] fabricated the FG Al–Cu–Mg alloy reinforced with 5 wt% SiC particles obtained by centrifugal casting process to study mechanical and wear behaviour. Experimental results showed that there was increased concentration of SiC particles at outer zone. so, the mechanical properties and wear resistance increased at this zone. Results from the microstructure show that the outer zone of FG sample was more particle concentration than the transition and inner zone. Figure 11 shows the distribution of particles along with radial distance from outer to inner zone.

Recently, Jayakumar et al. [95] investigated the influence of reinforcement content of FG A319 alloy reinforced with 20 wt% SiC particles fabricated through centrifugal casting process to analyse the microstructure and wear behaviour at different parameter. The results of the microstructure analysis show that the particles are distributed continuously along with the radial distance of FG composite thickness as illustrated in Fig. 12. The SiC particles addition successfully improved the mechanical properties and wear resistance compared with A319 alloy (matrix material).

2.2 Aluminium Oxide Reinforced FGAMCs

Alumina (Al_2O_3) has a strong ion inter-atomic bonding that creates its necessary FGAMCs properties [24, 96]. in addition to SiC particles, aluminum oxide in its different levels of purity is used as reinforcement for FGM more often than any other ceramic materials, due to its advantages like very good insulation, moderate to extreme mechanical characteristics and high resistance to corrosion and wear [97, 98]. Also, the products of FG Al–Al_2O_3 are widely used in several engineering applications such as in rocket nozzle, wings, rotary launchers, heat shield systems, connecting rods, pistons, engine casting and gas turbines components [99]. Therefore, aluminum oxide material gained considerable emphasis to the researchers while manufacturing FGAMCs and many studies were carried out to examine the mechanical and wear properties of Al_2O_3 strengthened FGMs to ensure effective use of FGAMCs.

Prasad and Chikkanna [100] analyzed the mechanical and fractural properties of FG Al 6061 alloy with 20 wt% of Alumina particles obtained by centrifugal casting technique. Resulting from the microstructures, the outer zone FG

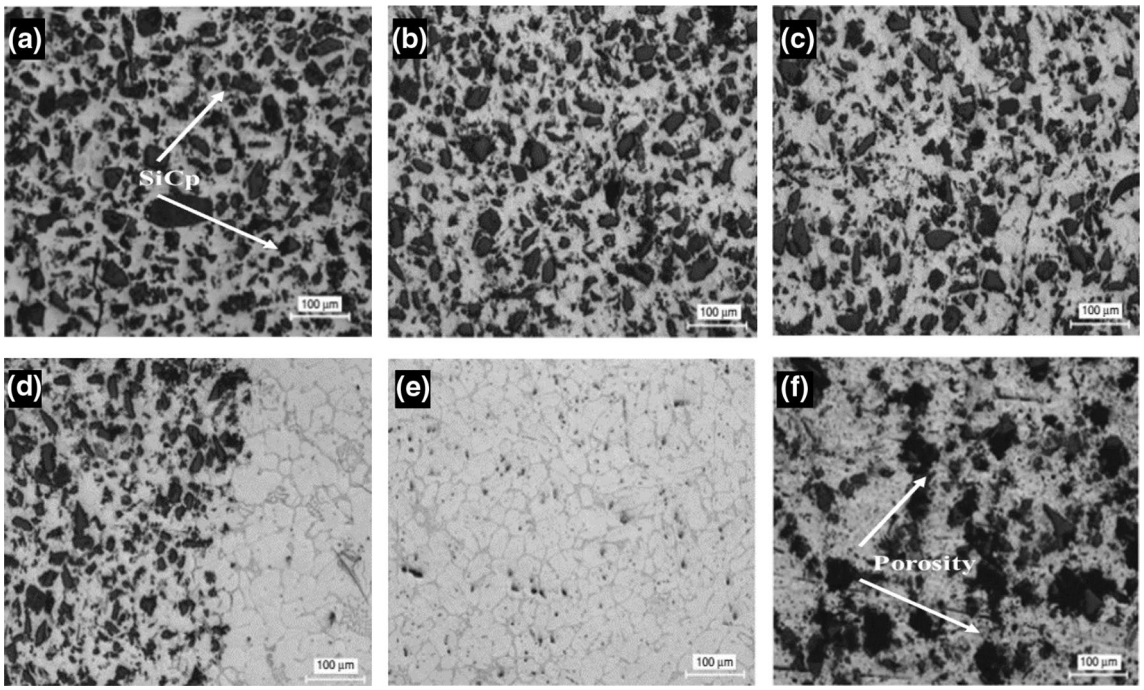

Fig. 11 Microstructures of the FG Al alloy/SiC_p at various locations from outer to inner zone. **a** 1 mm, **b** 3 mm, **c** 4 mm, **d** 7 mm, **e** 15 mm and **f** 55 mm [94]

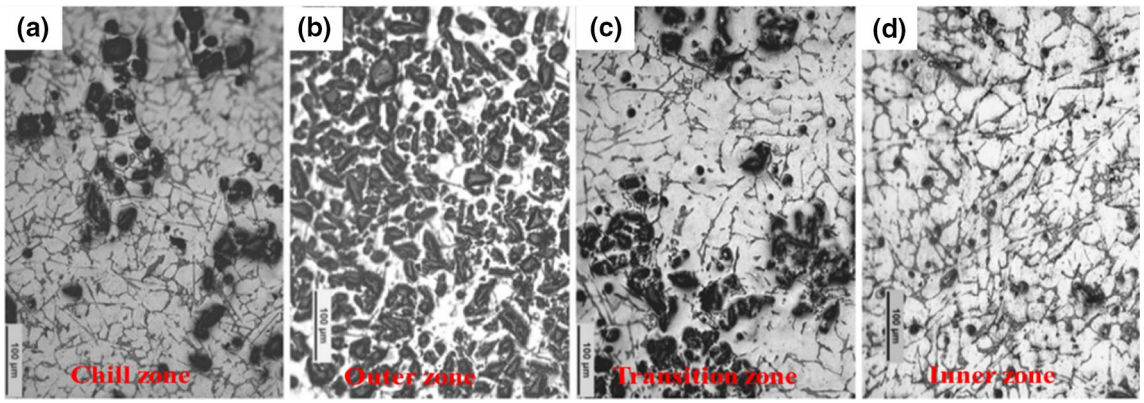

Fig. 12 Microstructures of the FG A319 alloy/SiC_p from the outer to inner zone. **a** Chilling zone, **b** outer zone, **c** transition zone and **d** inner zone [95]

composites is more particle concentrations than the transition and inner zones. They found that the addition of Al_2O_3 improves hardness and compression of FG Al6061–Al_2O_3 composites but reduces ductility.

Junus and Zulfia [101] investigated the mechanical properties of FG Al alloy reinforced with three different volume fractions (3,5 and 10 vol%) of Alumina particles produced by centrifugal casting method. According to results of microstructure, the presence of Alumina particles on the outer zone has improved the properties as shown in Fig. 13. Figure 13a shows the particle distribution in the different zones (outer, transition and inner) across the wall thickness of the FGM pipe. Figure 13b indicates the transition zone-outer zone interface. while, Fig. 13c illustrates the distribution of particles in the outer zone, and shows the existence of some particle agglomeration in this zone.The findings also showed that the mechanical characteristics of the FGM pipes are improved when the amount of reinforcement alumina increases, as shown in the results in table at the end of section 2.

Recently, Saleh and Ahmed [102] investigated the mechanical properties and wear behaviour of FG pure Al

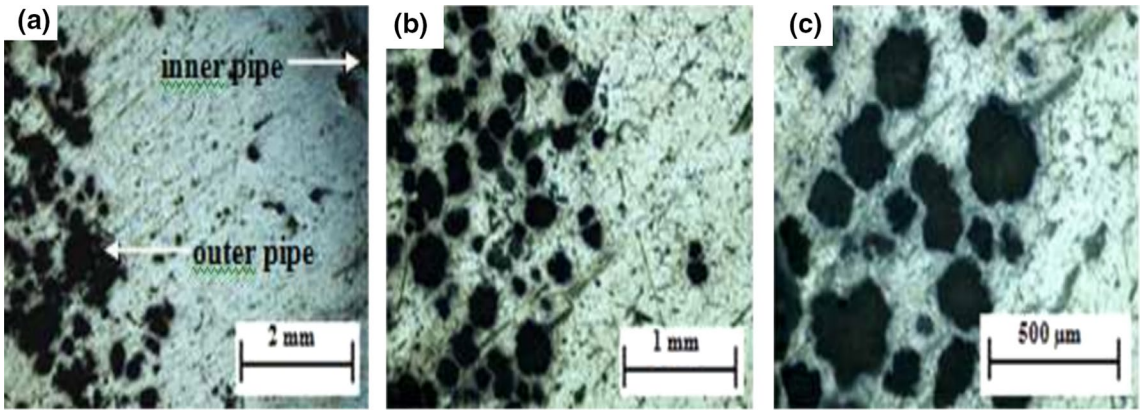

Fig. 13 Microstructure of FG Al/Al2O3 composite at different magnification: **a** ×50, **b** ×100 and **c** ×200 [101]

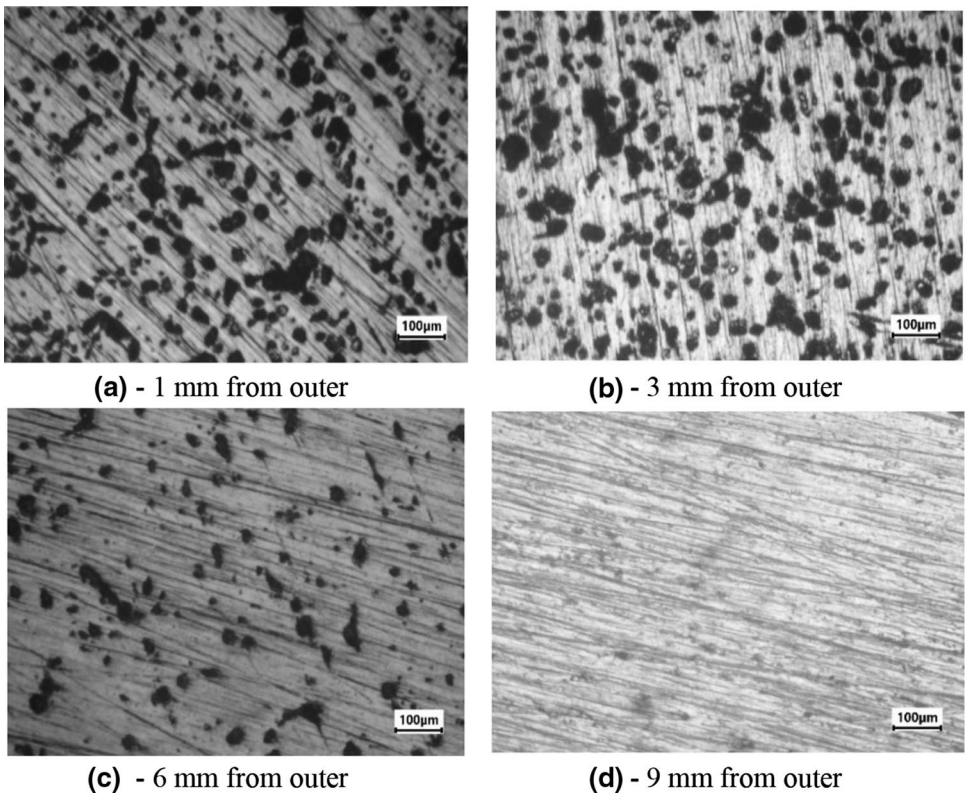

Fig. 14 Microstructure of FGM with 10 wt% Al_2O_3 particles of 16 µm [102]

reinforced with three different weight fractions (2.5, 5 and 10 wt%) of Alumina particles produced by centrifugal casting method. According to results of microstructure, the presence of Alumina particles on the outer zone has improved the properties as shown in Fig. 14. The findings also showed that the mechanical characteristics and wear resistance of FG Al 1010 reinforced with Al_2O_3 particles composites was much superior at outer zone compared to other particles, as shown in the results in table at the end of section 2.

2.3 Titanium Carbide Reinforced FGAMCs

Due to its attractive properties including high hardness, high wear and extremely high corrosion resistance, titanium carbide (TiC) is one of the most promised ceramic materials [56]. TIC is widely used as reinforced materials for FGMs systems in numerous engineering applications including bearings, cutting tools, thin film ultracapacitors, cermet components, nozzles, wear and corrosion resistant applications, etc. [103].

Various researchers have reported that reinforcement parameters of FGAMCs obtained by centrifugal casting system has a major influence on the properties of products which could be optimized. But, to the best of our knowledge, no work or limited research is done on FG Al alloys reinforced with TiC particles, so It needs further research to explore further [104].

Radhika and Raghu [105] investigated the mechanical and wear characteristics of FG LM 25 alloy reinforced with 10 wt% of TiC particle fabricated via horizontal centrifugal casting method at constant mould speed 1200 rpm. Adding TiC particles enhances mechanical properties of the FGAMMC tubes and their wear resistance specially at outer zone. The wear resistance increased linearly with increase in TiC content across the FGAMCs tube thickness and decreased with increase in applied load and sliding speed.

Ramkumar et al. [106] investigated the effect of FG four various weight fraction (0, 2.5, 5 and 7.5 wt%) of titanium carbide particle reinforced AA 7075 MMC at various process conditions on mechanical and tribological properties. The results have shown that when the weight fraction of TiC particles increases, the mechanical and tribological characteristics of composites increase. In case 7.5 wt%, a composite agglomeration of TiC particles due to the high particles contents was observed.

2.4 Boron Carbide Reinforced FGAMCs

One of known hardest materials behind diamonds and cubic boron nitride is boron carbide (B_4C). B_4C is used as reinforcement for FGM due to its properties like low density, extreme hardness, good chemical resistance and good nuclear properties [107]. The major problem of developing B_4C reinforced FGAMCs is the agglomeration of the B_4C particles and their homogeneity in the base metal. Therefore, the B_4C reinforced FGAMCs produced by centrifugal casting need more investigation by researchers.

Rao et al. [108] developed AA6061 alloy reinforced with 10 wt% of B_4C particles (25 µm avg. size) were obtained by centrifugal casting method to determine these graded properties at two different mould rotational speeds. The difference in density between AA6061 alloy (2385 kg/m^3) and B_4C (2520 kg/m^3) has been investigated for manufacturing FGAMCs with continuous gradients, based on the effect of the centrifugal force due to rotational speed. The results showed, in comparison to base metal especially in outer zone, that the mechanical characteristics of FGAMCs increased with an increase in particle concentration in B_4C.

Radhika and Raghu [109] investigated the abrasive wear resistance of FG Al–Si12–Cu alloy reinforced with 10 wt% of B_4C particles (33–40 µm avg. size) were obtained via centrifugal casting method at constant rotational speed 1000 rpm. According to the microstructure results as shown in Fig. 15, the centrifugal force led to the movement of the boron carbide particles to the outer zone of the FG composites, and the concentration of particles decreased when moving from outer to inner zone. The presence of B_4C particles on the outer zone has improved the wear resistance.

2.5 Zirconia Reinforced FGAMCs

Zirconia, consisting principally of ZrO_2, has the highest mechanical strength and robustness to fractures in all major fine ceramics at room temperature. It is used to make blades, scissors and knives for cutting. Due to its superior surface smoothness, it is used for pump parts too. Zirconia is used as reinforcement for FGM due to its properties like high thermal expansion, excellent thermal insulation, low thermal conductivity, high fracture toughness and very high resistance to crack propagation [110].

Radhika and Raghu [111] investigated the mechanical, wear behaviour and examined the microstructure of FG Al alloy reinforced with 10 wt% zirconia developed by horizontal centrifugal casting method. It was observed that enhancement in mechanical characteristics and wear resistance of FGM composites due to the presence of strong content of ZrO_2 particles. Also due to high density of zirconium dioxide particles (5680 kg/m^3) compared to density of Al–Si12Cu alloy (2700 kg/m^3), there was agglomeration of particles at outer zone of FGM composites as shown in Fig. 16. The wear resistance of FGM composites improved by 43% and 23% at outer and middle zones respectively, compared with unreinforced alloy. In 2016 they extended their work and studied the mechanical and wear behaviour with the variation of applied load and sliding speed [112]. horizontal centrifugal casting technique was developed to fabricate the FG Al LM 25 alloy reinforced with 15 wt% zirconia at 1200 rpm. It was observed that Wear resistance improved due to the high content of zirconium dioxide particles. With increase in the applied load, the wear resistance is observed to decrease.

Recently, Jojith and Radhika [113] studied the investigated of reinforcement particles type on the mechanical characteristics and wear rate of FG Al alloy reinforced with 10 wt% of B_4C, SiC and ZrO_2 particles obtained by centrifugal casting process at 1500 rpm. It was proved that the mechanical characteristics and wear resistance of FG Al 12Si–Cu reinforced with ZrO_2 particles composites was much superior at outer zone compared to other particles.

2.6 Other Particles Reinforced FGAMCs

Some of the reinforcement particles, for example WC, TiS_2, Si_3N_4 and AlB_2 are not extensively used in the fabrication of FGAMCs, mainly because of several aspects such as production methods, costs or the difficulty of obtaining a smooth gradient and finding a suitable application of these materials after manufacturing. These particles require more attention and

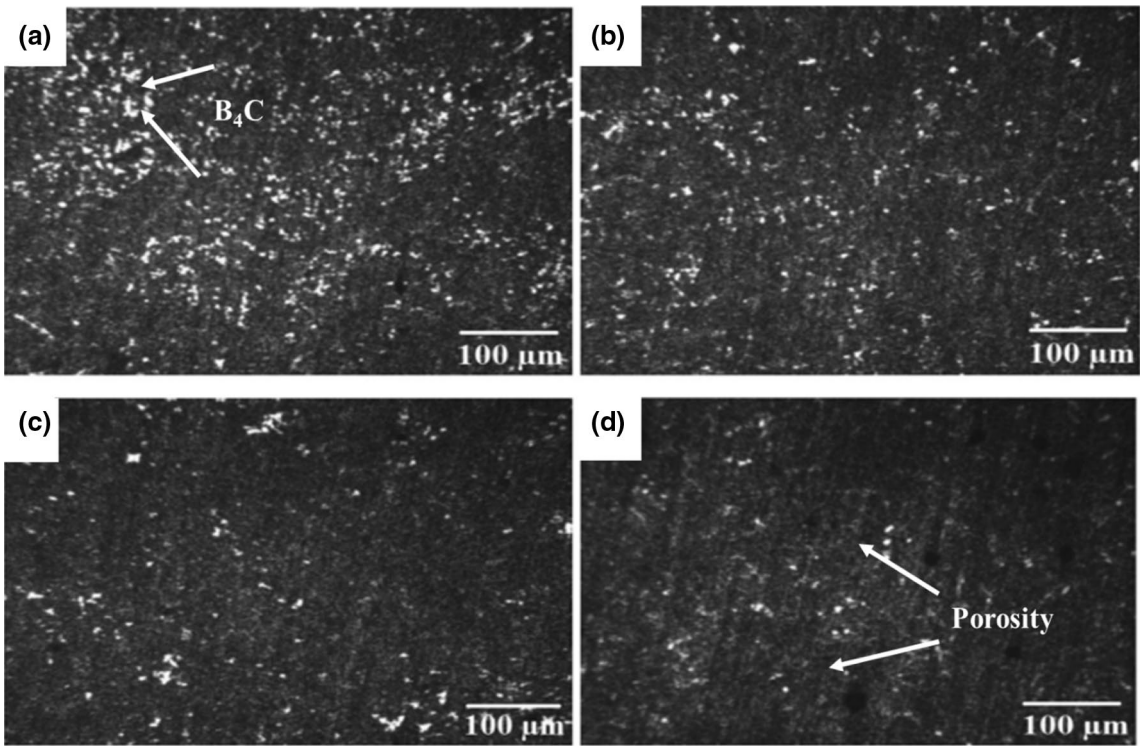

Fig. 15 Microstructures of the FG Al alloy/B_4C at various locations from outer to inner zone. **a** 3 mm, **b** 6 mm, **c** 9 mm, and **d** 11 mm [109]

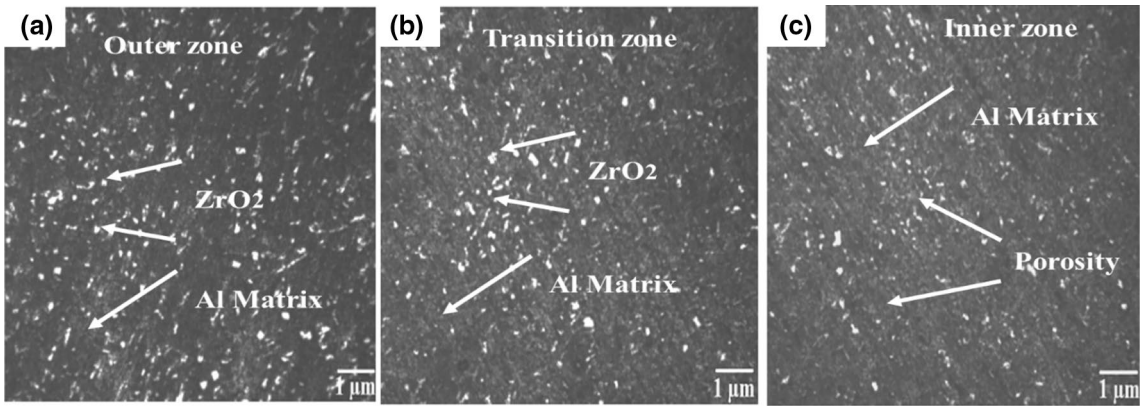

Fig. 16 Microstructures of the FG Al alloy/ZrO_2 composite at different zones. **a** Outer zone, **b** transition zone and **c** inner zone [111]

research and therefore, the available experimental findings of these reinforcement particles are discussed in this sub-section.

Radhika and Raghu [114] studied the results of an experimental investigation of the wear behaviour of FG LM 25 alloy reinforced with 10 wt% of aluminum diboride (AlB_2), processed by centrifugal casting route at 1200 rpm. There was gradient of particles from outer to inner zone through the thickness of FGM composites as shown in Fig. 17. It was found that the wear resistance of the FG LM 25–10 wt% AlB_2 composites increases at outer zone, due to high content of particles in this zone, as shown in the results in table at the end of section 3. In 2016 [115] they extended their work and investigated the influence of particle size on mechanical and wear behaviour of FG LM 25–10 wt% AlB_2 composites. Three different aluminum diboride particle sizes (15, 44 and 74 µm) were examined. The results have shown that the outer wear rate is decreasing with the particle size increasing.

Jojith and Radhika [116] studied the mechanical and wear behaviour and analyzed the microstructure of FG LM 25 alloy reinforced with 10 wt% of tungsten carbide (WC) developed by horizontal casting method. Although the density difference between the LM 25 (2700 kg/m^3) and the

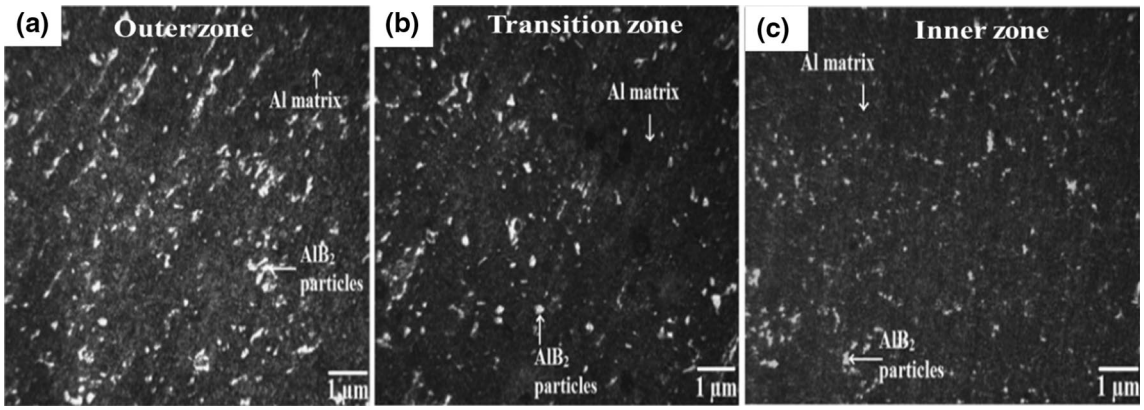

Fig. 17 Microstructures of the FG Al alloy/AlB_2 composite at different zones. **a** outer zone, **b** transition zone and **c** inner zone [114]

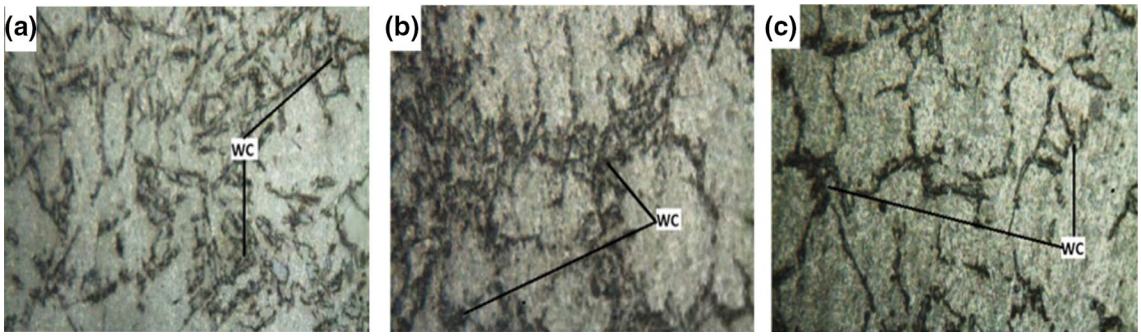

Fig. 18 Microstructures (×200 magnification) of the FG LM 25 alloy/WC at various locations from outer to inner zone. **a** 1 mm, **b** 11 mm and **c** 18 mm [116]

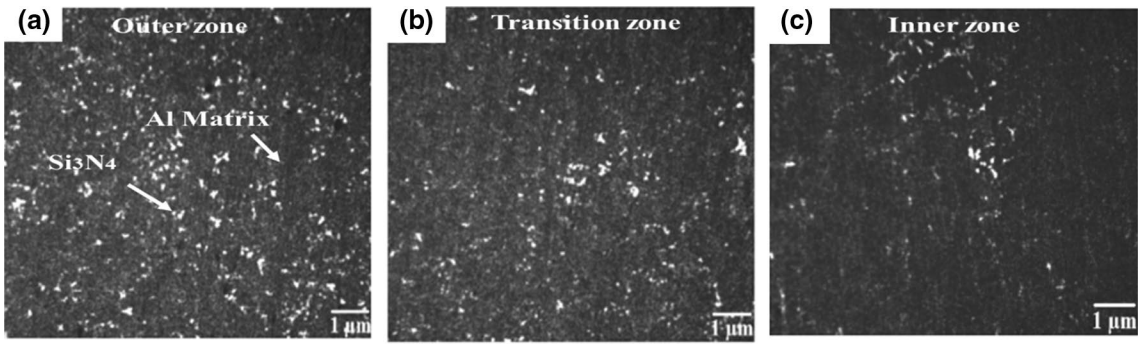

Fig. 19 Microstructures of the FG LM 25 alloy/Si_3N_4 composite at different zones. **a** Outer zone, **b** transition zone and **c** inner zone [117]

tungsten carbide particles (15,600 kg/m^3) is very large, the results showed a continuous gradient with localized agglomeration of particles at some places as shown in Fig. 18. Addition of WC particles improved the wear resistance of the FGAMCs. The wear resistance of FG tubes enhanced by 44% outer zone compared to unreinforced alloy.

Radhika [117] studied the mechanical and wear behviour of FG LM25 alloy reinforced with 10 wt% of silicon nitride particles fabricated by centrfiugal casting method at 1250 rpm. The results demonstrated the high content of particles in the outer zone of FG composites as compared with the transitional and inner zones as described in Fig. 19. The wear resistance decreased with the applied load increases at all zones.

Table 1 summarizes the main parameters and applications of the functionally graded aluminum matrix composite (FGAMC) systems used in this research.

Table 1 Literature survey of production parameters and applications for FGAMC systems obtained by centrifugal casting process

FGM system	Production parameters				Extent of mechanical properties improvement over matrix at outer zone (%)		Study	FGM system applications	Refs.
	Process parameters		Reinforcement characterisation						
	Speed (rpm)	Pouring temp (°C)	Size (μm)	Weight fraction (wt%)	Hardness	Tensile			
Al6061/SiC_p	1300	–	100	20	43	17	Influence of particles wt% on microstructure and mechanical behaviour	Cylinder liners and connecting rod	[87]
Al–Si alloy/SiC_p	1800	760	15	20	–	–	Effect of particles size on microstructure behaviour	Advanced electronic packaging industry	[88]
			30						
			59						
Al 356/SiC_p	1100	750–760	23	15	42	–	Effect of matrix type on mechanical properties	Fly wheels and racing car brakes	[89]
Al 2142/SiC_p					22				
Al–10Si–4.5Cu–2 Mg alloy/SiC_p	1500	850	37.8	10	37	–	Effect of mould speed on gradient of particles, wear rate and hardness	Automotive applications	[90]
	2000				23				
Al 356/SiC_p	1200	760	23	20	44	–	Influence of process parameters on wear and hardness	High surface wear applications	[91]
Al 359/SiC_p	700	750	16	20	11	15.6	Effect of rotational speed on mechanical properties	Automotive and aerospace applications	[92]
	1300				19	–			
Al6061/SiC_p	1300	780	23	10	36	–	Hardness and wear measurement of different zones of composite	High surface wear applications	[93]
Al–Cu–Mg alloy/SiC_p	600	750	20	5	38	–	Effect of low speed on mechanical and wear properties	Cylinder liners	[94]
Al 359/SiC_p	1300	760	23	20	66	–	Hardness and wear measurement of composite	High surface hardness applications	[95]
Al6061/Al_2O_3 particles	530	750	30–50	5	–	21	Influence of weight fraction on microstructure behaviour and tensile properties	Rocket nozzle and rotary launchers	[100]
				10		29			
				15		29.4			
				20		31.4			
Al6061/Al_2O_3 particles	800	800	63	5	25.5	–	Hardness measurement at different zones of composite	Piping and marine applications	[101]
Al1010/Al_2O_3 particles	800	725	16	10	34	17	Effect of weight fraction on mechanical and wear behavior	Cylinder liners and tubes	[102]
	900				38	23			
	1000				41	34			
LM 25 alloy/TiC_p	1200	–	25	10	32	–	Hardness and wear measurement of composite	Cylinder liners and bearing	[105]
Al6061/B_4C_p	600	900	25	10	7	–	Hardness measurement at different zones of composite	Piping systems	[108]
	1100				13				

Table 1 (continued)

FGM system	Production parameters				Extent of mechanical properties improvement over matrix at outer zone (%)		Study	FGM system applications	Refs.
	Process parameters		Reinforcement characterisation						
	Speed (rpm)	Pouring temp (°C)	Size (μm)	Weight fraction (wt%)	Hardness	Tensile			
Al–12Si–Cu alloy/B_4C_p	1000	–	33–40	10	15	–	Effect of B_4C particles on three-body wear behavior	Cylinder liners	[109]
Al–12Si–Cu alloy/ZrO_2	1300	–	50	10	37	15	Hardness, tensile and wear measurement of composite	Automotive applications	[111]
LM 25 alloy/ZrO_2	1200	–	50	15	37.5	–	Effect of ZrO_2 particles on hardness and wear behavior	Automotive applications	[112]
Al–12Si–Cu alloy									
ZrO_2	1500	760	20	10	39	–	Effect of particles type on hardness and wear behavior	Automotive bearings, piston rings, and brake drums	[113]
SiC_p			10		22				
B_4C_p			20		18				
LM 25 alloy/AlB_2	1220	–	33	10	32	11	Effect of particles size on mechanical and wear behavior	Cylinder liners, brake drum and pistons	[115]
			44		37	14			
			74		40	18.9			
LM 25 alloy/WC_p	1000	760	–	10	46	45	Effect of WC particles on mechanical and wear behavior	Pistons, bearings and brake drum applications	[116]
LM 25 alloy/Si_3N_4	1250	–	40	10	32	14	Effect of Si_3N_4 particles on mechanical and wear behavior	Cylinder blocks and heads	[117]
Al7075/SiC_p	700	780	7–34	7.5	28	11	Influence of weight fraction on mechanical characteristics and wear behaviour	Brake rotors and cylinders	[136]
				9.5	35	14			
Al1010/SiC_p	1000	725	16	10	46	28	Influence of particle size on distribution of particles, mechanical and wear behaviour	Cylinder liners, and diving cylinders	[127]
			23		44	26			
			500		41	20			
Al 2014/SiCp	2650	700	9	15	35	27	Effect of particles size on mechanical and wear behavior	Fly wheels	[137]
A390/Mg	800	760	–	0.5	24	–	Effect of Mg content on mechanical and wear behavior	Automotive piston	[138]

3 Influence of Wear Test Parameters on Wear Properties

Wear characteristics are important functional parameter which is extremely important when designing and selecting materials for machine and mechanism components that have a relative motion between them to produce either a sliding or rotating contact surface [118]. The wear test is performed to assess a material's wear characteristic in order to determine whether the material is appropriate for a wear application and to evaluate the potential of using a technique for surface engineering to reduce wear on a specific application, as well as to investigate the impact on wear performance of the treatment conditions, process and material parameters [119]. Also, the implementation of this test is mainly due to the large number of engineering applications requiring high wear resistance [120].

Wear test of FGAMCs has many parameters that affect the wear properties such as applied load, sliding distance, sliding speed, duration of test and the temperature (Fig. 20) [121]. Therefore, in the following sub-sections the relation between wear rate, reinforcement particles and these parameters are summarized.

3.1 Influence of Applied Load on Wear Rate

Applied load exerts a major role on the mode of wear rate and needs to determine partly in relation to resistance required. Jayakumar et al. [122] investigated the wear performance and analyzed the microstructure of FG A319–10 wt% SiC_p with particle size 23 µm developed by vertical centrifugal casting technique. Wear tests were performed at an applied load of 10–40 N with sliding speed of 2 m/s and time of 15 min. Microstructure results reveal the distribution and concentration of SiC_p between the outer and inner zones within the matrix compared to unreinforced A319 alloy. The FG A319- 10 wt% SiC_P rings at the outer zone improved the wear resistance by 39% compared with the inner zone. Figure 21 shows SEM images of surface worn for FG A319–10 wt% SiC_p specimens at different magnifications. The wear resistance decreased linearly with increase in applied load in wear test as shown in Fig. 22.

Radhika and Raghu [123] investigated the mechanical and wear properties of Al–12Si–Cu alloy reinforced 12 wt% SiC, TiB_2,Al_2O_3 and B_4C particles at constant mould rotational speed 1300 rpm using centrifugal casting fabrication technique. Results of Microstructure revealed that the outer zone of all FGAMCs exhibit higher concentration of particles than other the transition and inner zones and thus increased the properties of FGAMCs at this zone. Wear tests were performed at an applied load of 20–80 N with sliding speed of 50–200 rpm and time of 3–9 min. Figure 23 shows the effect of different loading conditions and type of reinforcement on wear rate for FGAMCs. The wear resistance was less at outer zone in case of FG Al/B_4C compared with other FG composites. Figure 24 shows SEM images of Al/B4C specimens at different loading condition.

Recently, Jayakumar et al. [95] studied the wear behaviour of FG A319 alloy-20 wt% SiC particles prepared via centrifugal casting technique at different applied load. Four different applied loads (1, 2, 3 and 4 kg) were used at constant sliding velocity 2 m/s. Experimental result illustrated that the wear rate was increased with increasing applied load in both FGAMCs and unreinforced alloy. Figure 25 shows the effect of applied load on wear rate for FGAMCs and A319 alloy at different zones.

Radhika and Raghu [124] investigated statistically the effect of wear parameters such as applied load (28, 40 and

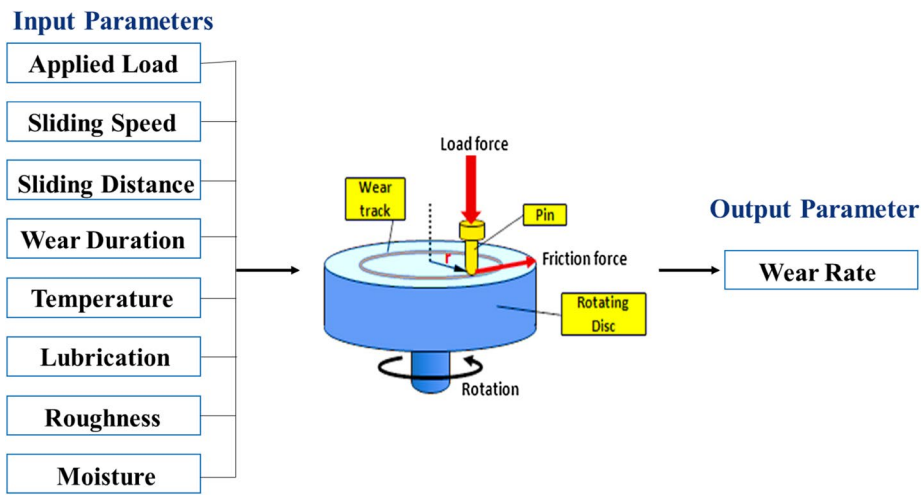

Fig. 20 Example of pin on disk apparatus with wear testing parameters

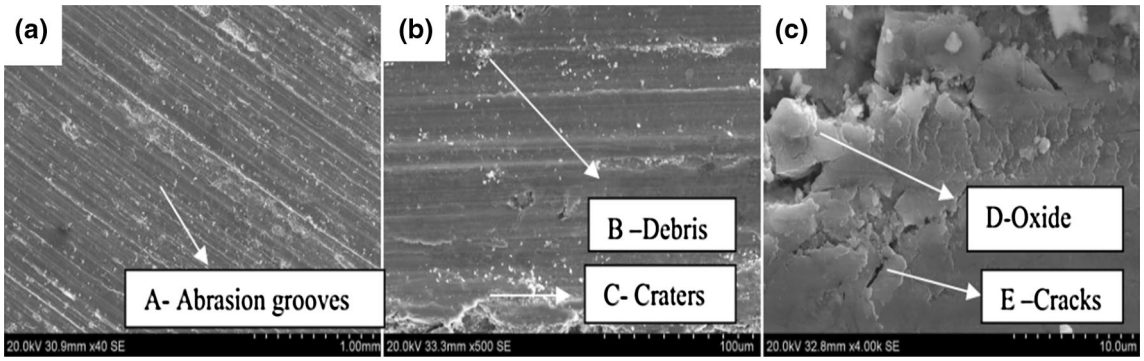

Fig. 21 SEM image of the FG A319 alloy/SiC pins at various magnifications. **a** ×40, **b** ×500; **c** ×4000 [122]

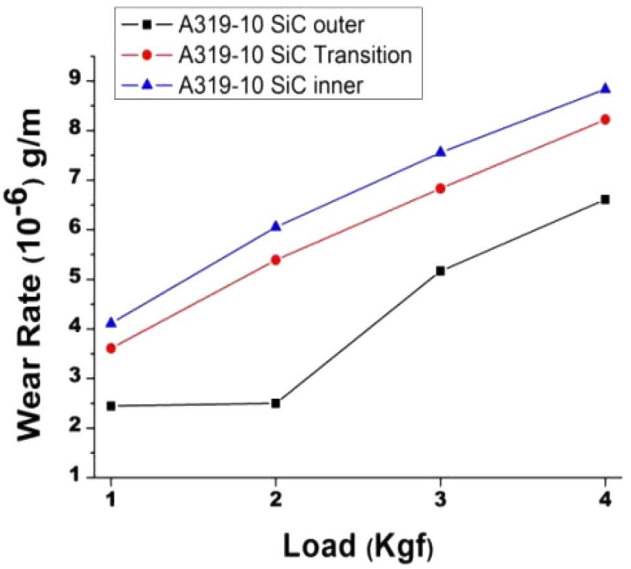

Fig. 22 Effect of applied load on wear rate of FG A319/10 wt% SiC at different zones [122]

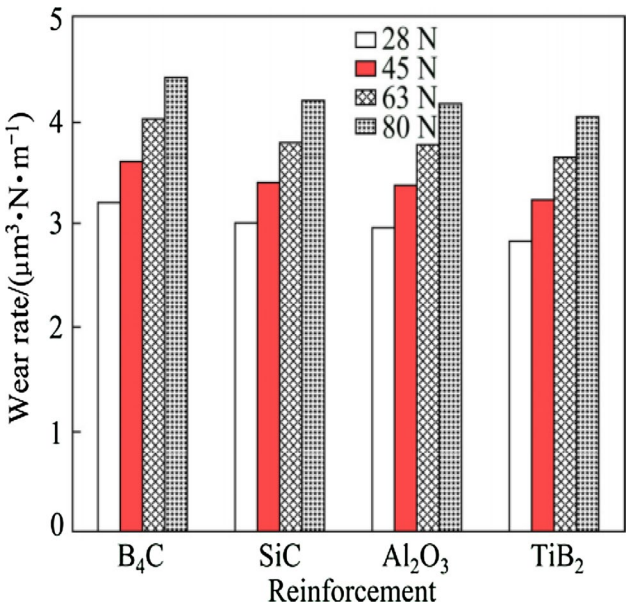

Fig. 23 Influence of reinforcement type on wear rate of FGMs [123]

52 N) and sliding speed (100, 150 and 200 rpm) of three body abrasion wear sliding behaviour of FG Al–Si_5Cu_3 alloy reinforced with 10 wt% of B_4C particles via centrifugal casting. The authors concluded that load in the most important factor affecting the wear rate of the FG tube followed by sliding speed. The weight loss increased with increase in load and sliding distance. Figure 26 shows SEM images of surface worn for FG A319–10 wt% B_4C particles at 15 mm from outer zone with different loads.

3.2 Influence of Radial Distance on Wear Rate

The radial distance across thickness is very important given the smooth gradient of FGM properties, since it manages product characteristics in one way or another and thus also defines the type of application of these materials.

Radhika [125] analysed statistically the wear characteristics at different wear test parameters of FG LM 13 alloy reinforced with combined 10 wt% titanium disulphide (TiS_2) particles. The author observed, with increasing load and sliding distance, that wear rate of the FG tube increased, while the wear rate decreased with increased sliding speed. The results also demonstrated that the wear resistance decreased as the radial distance from the FG tube from the outer to the inner zone was increased. Because of the high concentration of TiS_2 particles towards the outer zone, which is originally due to the high centrifugal force compared to other zones. Figure 27 shows the worn surfaces of samples at different radial distance of tube. As demonstrated in Fig. 27a, the sliding wear in the outer zone of the FGM tube has decreased significantly, then started again to rise as a result of the

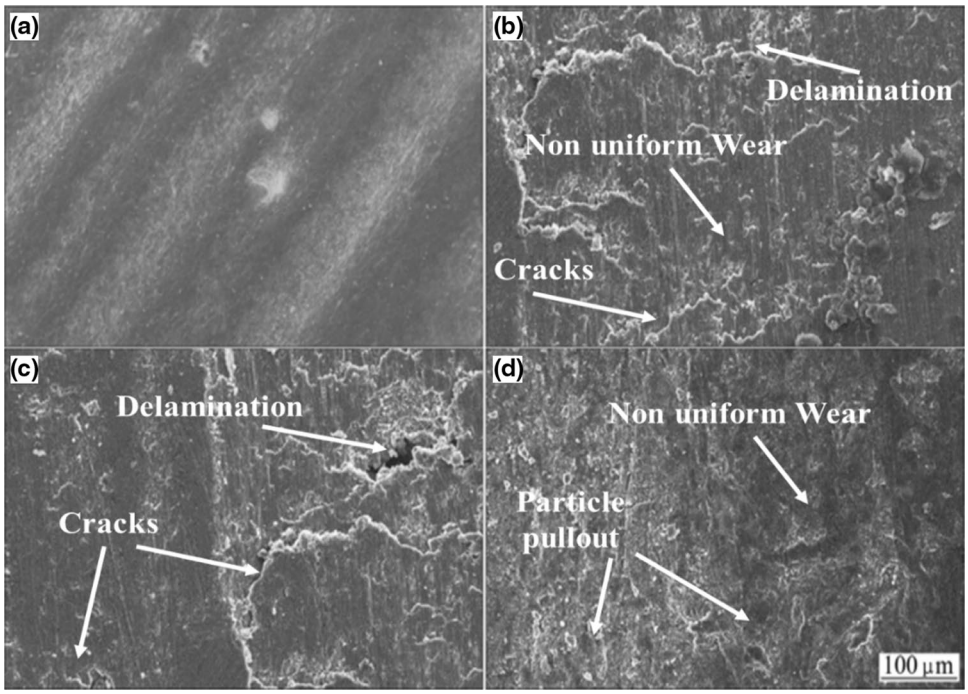

Fig. 24 SEM images of FG Al/B_4C composites at different loads **a** 28 N, **b** 45 N, **c** 63 N and **d** 80 N [123]

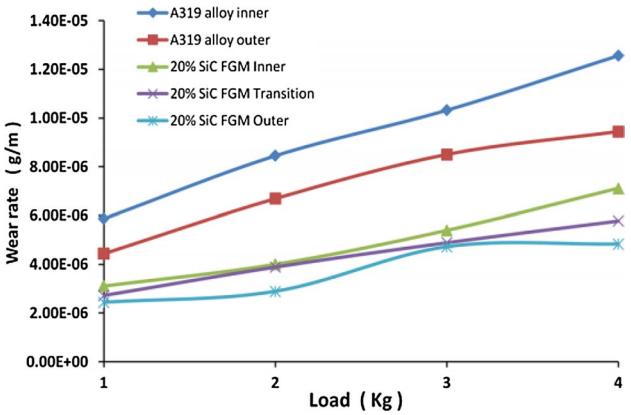

Fig. 25 Influence of applied load on wear rate of FG Al alloy/10 wt% B_4C at different zones [95]

decrease in the concentration of particles in other zones as shown in Fig. 27b, c.

The wear behaviour of FG Al–Si5Cu alloy reinforced with 10% B4C particles (33 µm average size) obtained by horizontal centrifugal casting method have been investigated by Radhika and Raghu [126]. They found that the wear resistance in the FGAMCs increased respect to the unreinforced alloys. With increasing the applied load of wear test, the weight loss increased at all zones of FGAMCs. Figure 28 shows the effect of various loading conditions on wear rate at different distance from outer to inner zone.

El-Galy et al. [127] designed and manufactured the FG pure Al reinforced with 2.5 to 15 wt% of SiC_p produced through centrifugal casting method at different process

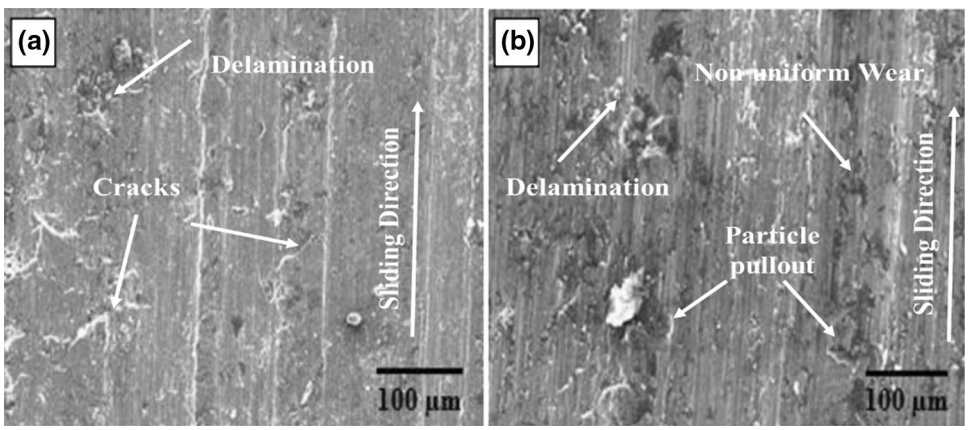

Fig. 26 SEM micrographs of the worn-out surfaces at different loads. **a** 28 N and **b** 52 N [124]

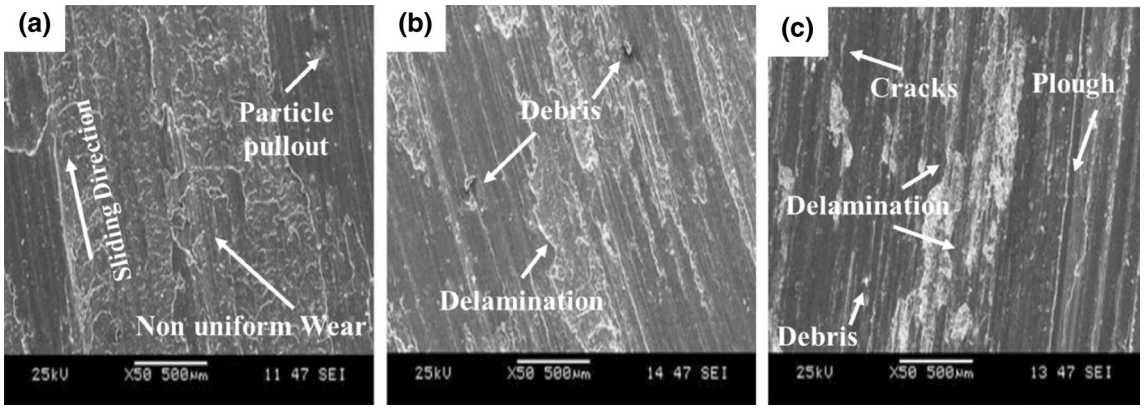

Fig. 27 SEM analysis of worn out surfaces at different distances with applied load 15 N and sliding distance 1500 m **a** 6 mm, **b** 15 mm and **c** 18 mm from outer zone [125]

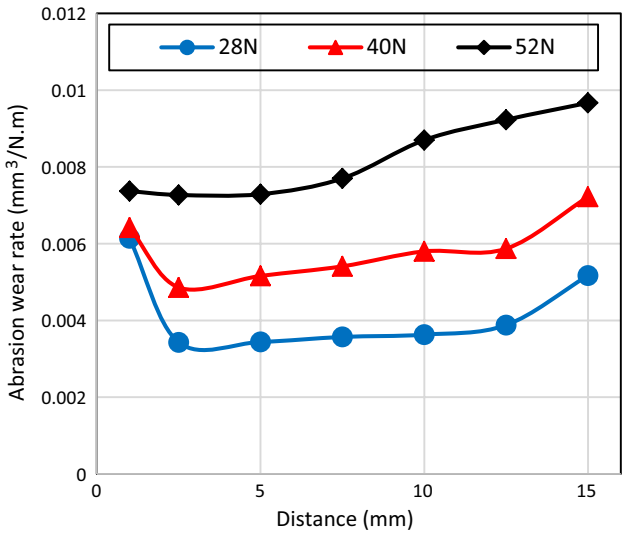

Fig. 28 Effect of different loads on abrasion wear rate at the constant speed of 200 rpm [126]

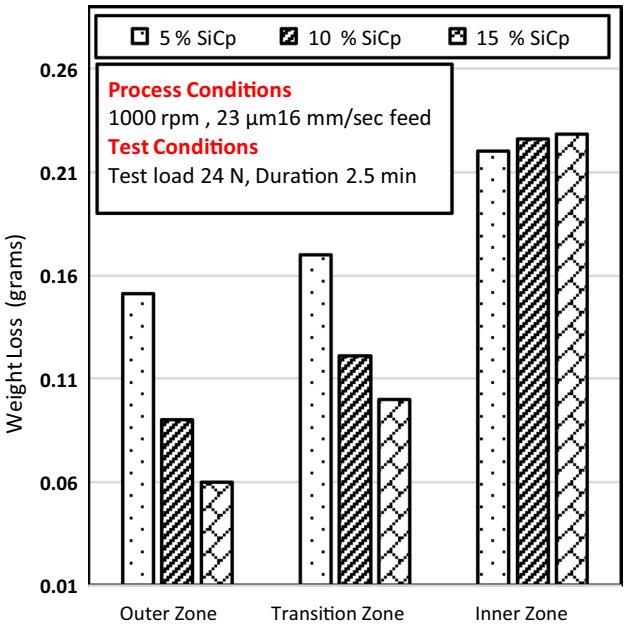

Fig. 29 Effect of weight fraction on weight loss at different zones [127]

parameters to evaluate mechanical and wear properties. Experimental results revealed that there was increased concentration of SiC particles with increasing weight fraction and mould rotational speed at outer zone. So, the mechanical properties and wear resistance increased at this zone. Microstructural findings showed that the outer zone of the FG tube was more concentration of particles than the transition and inner zones. Figure 29 shows the effect of weight fraction on weight loss at different zones.

3.3 Influence of Sliding Distance on Wear Rate

Several works on the effect of sliding distances and sliding velocities on wear behavior of FGAMCs have been reported. However, wear behavior under various test parameters still needs to be understood [129–130].

Jojith and Radhika [116] analysed the wear characteristics at different wear parameters of FG LM 25 alloy reinforced with combined 10 wt% WC particles. The authors observed that the wear rate of the FG tube increased with increase applied load and sliding distance, while the wear rate decreased with increase in sliding speed as shown in Fig. 30. The worn sample surfaces with varying sliding speed (1 m/s and 4 m/s) are shown in Fig. 31. The scratches and the deep grooves are mostly formed on the pin surface by WC particles, which increases the removal

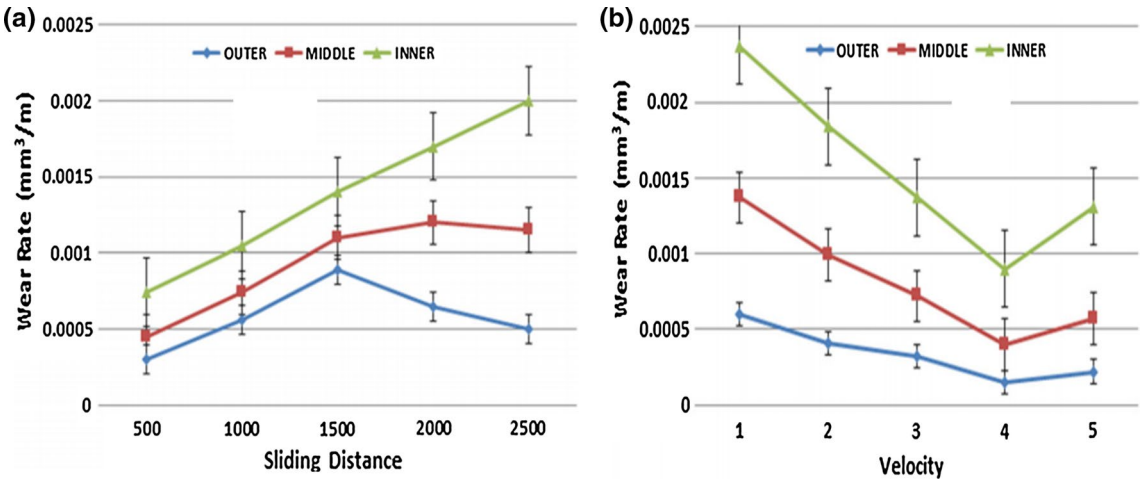

Fig. 30 Influence of wear test parameters on wear loss at different zones. **a** With sliding distance; **b** with sliding velocity [116]

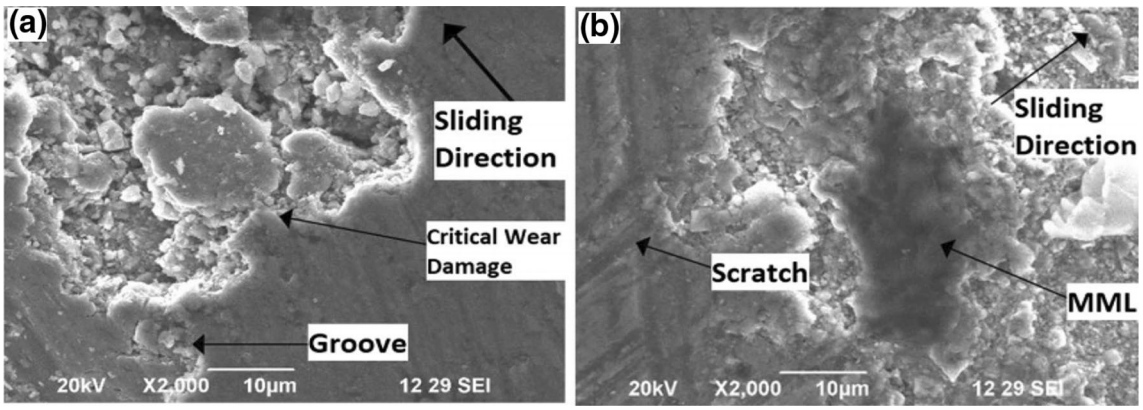

Fig. 31 Worn surface morphology of FG LM 25/WC with different velocities. **a** 1 m/s, **b** 4 m/s [116]

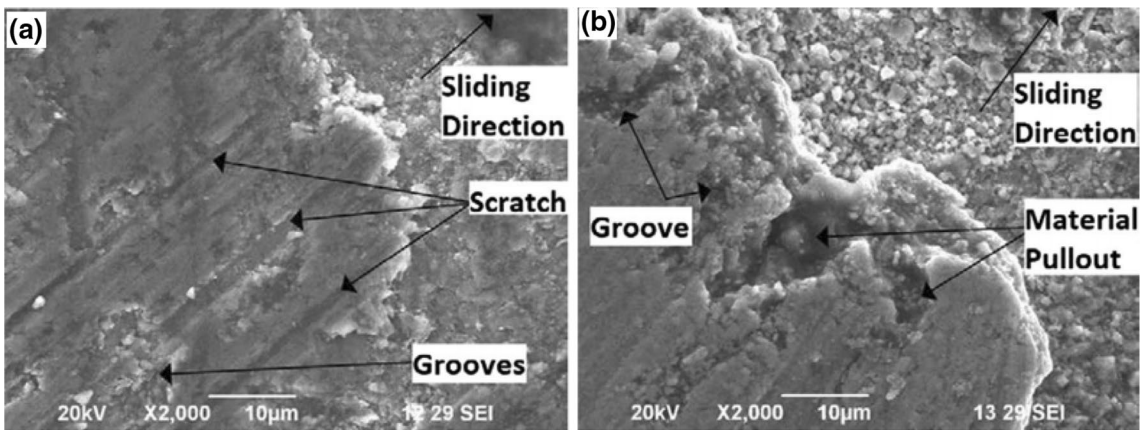

Fig. 32 Worn surface morphology of FG LM 25/WC with various distances. **a** 500 m, **b** 1500 m [116]

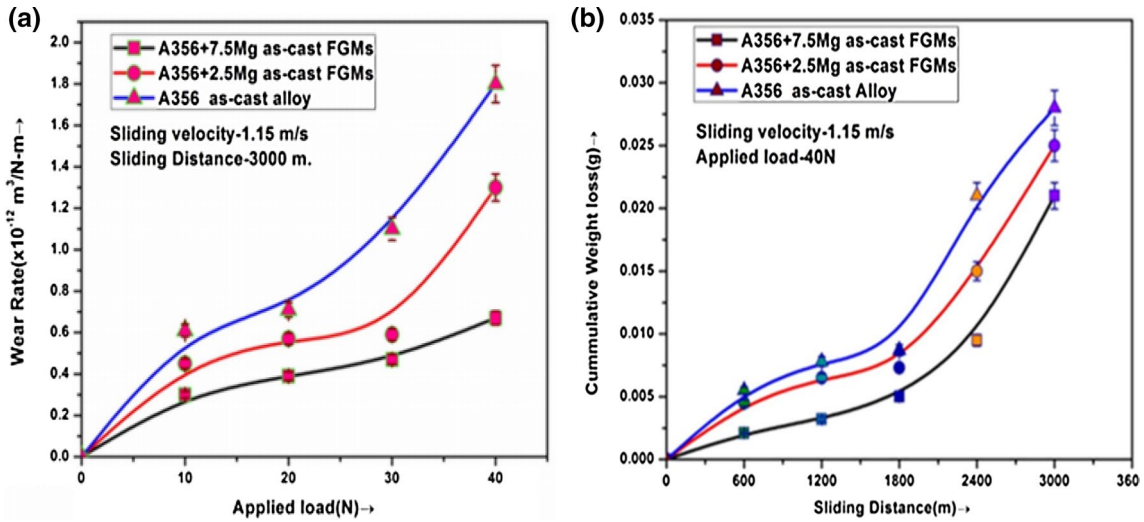

Fig. 33 Effect of wear test parameters on wear rate at different zones. **a** With applied load; **b** with sliding distance [131]

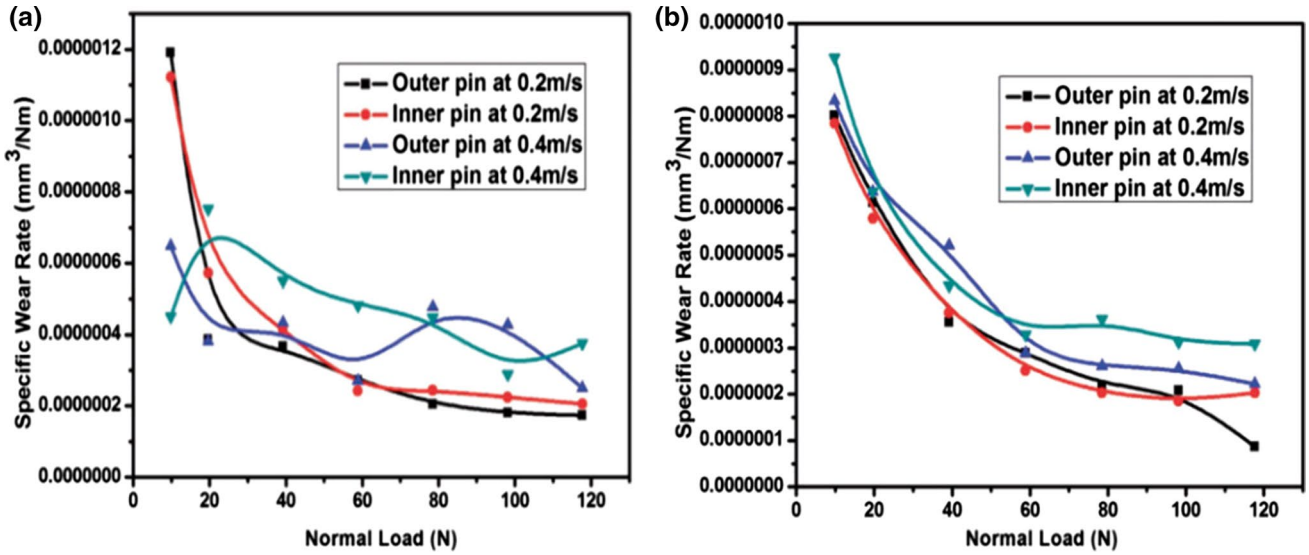

Fig. 34 Influence of sliding speed and weight fraction on wear rate values. **a** A356–10 wt% SiC and **b** A356–20 wt% SiC at velocities 0.2 and 0.4 m/s [132]

rate of material, with a low sliding speed (1 m/s) as shown in Fig. 31a. At a speed of 4 m/s (Fig. 31b), a thin glossy flake is formed on the wear track with plastically shaped grooves due to the mixture of debris produced by the micro cutting effect. The worn surface morphologies of the outer zone at different sliding distances are shown in Fig. 32, at the load applied as 30 N and sliding speed as 3 m/s. whisker scratches are observed on the sample surface at a low sliding distance of 500 m (Fig. 32a), as the particle-rich zone resists deformation forces. The minimum material removal rate and the trend is observed as a result of the very less time of contact between the sliding disk and the pin. High material removal rate is observed at 1500 m sliding distance (Fig. 32b), as deep grooves

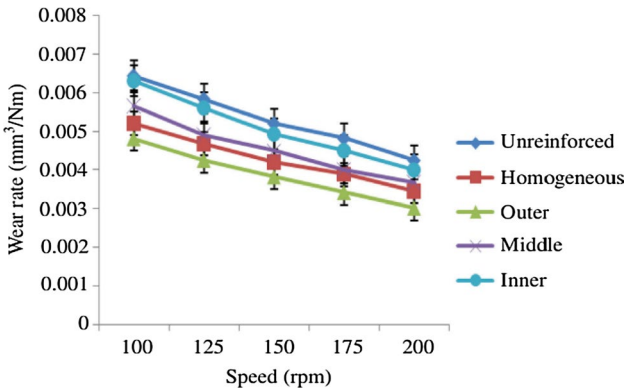

Fig. 35 Influence of sliding speed on the base alloy and FG tubes at load of 57 N [117]

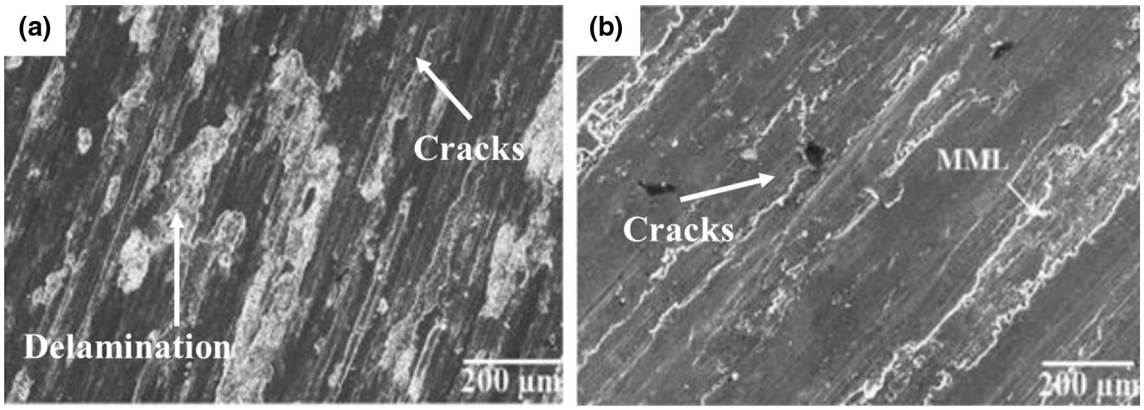

Fig. 36 SEM micrograph at different speed **a** 1.75 m/s **b** 3 m/s (at load 25 N and sliding distance 1200 m) [133]

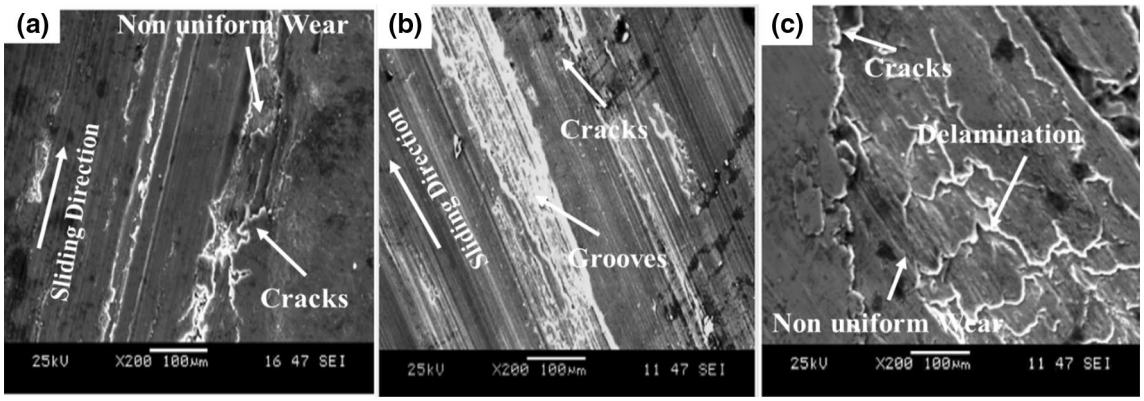

Fig. 37 SEM micrograph at different temperatures and applied loads with 1 m/s sliding speed. **a** 50 °C and 10 N; **b** 100 °C and 20 N; **c** 150 °C and 30 N [134]

and pull out of material, mainly because the increase in applied force and contact duration.

Ram et al. [131] investigated the influence of adding Mg and various wear parameters (applied loads and sliding distances) on wear behaviour of FG A356 alloy reinforced with Mg2Si. The authors concluded that the wear resistances of the FG composites increased compared with A356 alloy. The wear losses increased with increases the applied load and sliding distance for both FG and A356 alloy, but FG composite showed a lower rate of weight loss than that of matrix as shown in Fig. 33.

3.4 Influence of Sliding Speed on Wear Rate

Karun et al. [132] evaluated the wear rate on FG A356 matrix alloy reinforced with three different weight fractions (0 wt%, 10 wt% and 20 wt%) of SiC particles fabricated through centrifugal casting technique at 1300 rpm. the size of SiC particles was 23 µm. wear test parameters were at different loading conditions (10–120 N) with two sliding speed (0.2–0.4 m/s). Experimental results showed that with increased applied load both in FGAMCs and A356 matrix alloys, wear rate was increased. Figure 34 shows

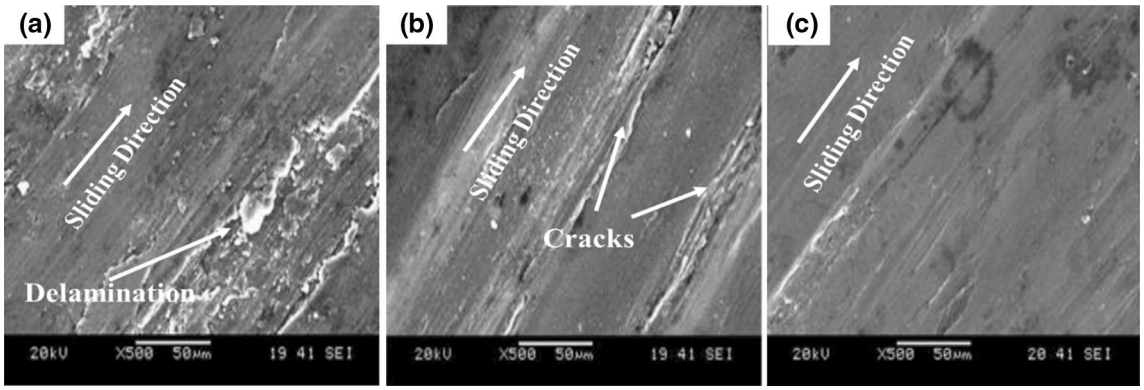

Fig. 38 SEM Micrograph at various aging times **a** 2 h; **b** 6 h; **c** 10 h [135]

the influence of load and speed on wear rate for FGAMCs and A356 alloy.

Recently, Radhika [117] studied and compared the mechanical and wear behaviour of FG LM25 alloy-10 wt% Si_3N_4 particles and homogenous composites prepared via centrifugal casting technique at different parameters. Experimental result illustrated that the wear rate was increased with increasing applied load in both FGAMCs, homogenous composites and unreinforced alloy. Figure 35 illustrations the influence of sliding speed on wear rate for FGAMCs, homogenous composite and LM25 alloy at constant load.

According to Radhika [133] the LM25 reinforced with 10 wt% of TiC particles possess higher mechanical properties and wear resistance, as compared with the base alloy. The results of the study revealed that the wear resistance increased, when TiC particles were added into the LM 25 alloy. The wear rate also decreased with increased speed as shown in Fig. 36.

3.5 Influence of Temperature and Heat Treatment on Wear Rate

Radhika et al. [134] investigated statistically the influence of wear parameters (load, sliding speed and temperature) on dry sliding behaviour of FG Al alloy reinforced with combined 9 wt% Al_2O_3 and 3 wt% graphite particles. The results revealed that the wear rate of the FG tubes is affected by load in the most important factor and sliding speed. With an increase in load and temperature, wear losses have increased as shown in Fig. 37. The wear results also revealed that the wear rate of the FG composites is low compared with AlSi10 Mg alloy.

Muddamsetty and Radhika [135] investigated the influence of heat treatment on sliding wear behaviour of FG LM13 alloy reinforced with 10 wt% of B_4C particles developed via centrifugal casting method. At different aging temperatures (150, 175 and 200 °C) and aging time (2, 6 and 10 h), the FG tubes were heat treatment for improving the property. 525 °C for 5 h solution treatment was done. The results revealed that wear rate of the both applied loads (10, 20 and 30 N) reduced drastically with increase in aging time (from 2 to 10 h) as shown in Fig. 38.

Table 2 provides a summary of wear research on the effects of wear test parameters in FGAMC systems obtained via the centrifugal casting process. The manufacturing parameters and applications of these systems are detailed in Table 1.

Table 2 Literature survey for FGAMC systems with main parameters of wear test obtained by centrifugal casting process

FGM system	Wear test parameters				Machine specs		Techniques and analysis		Max. extent of wear resistance improvement over matrix (%)		Refs.
	Load (N)	Sliding distance (m)	Time (min)	Sliding speed (m/s)	Apparatus	Counterpart	Techniques (modelling)	Analysis	Outer zone	Middle zone	
A319/20 wt%SiC_p	10–40	1800	12	2	Pin on Disk	EN 31	–	SEM	36–43	25–29	[95]
Al1010/x wt% Al_2O_3	24	–	0.5–3	8		EN 31	–	SEM	29–42	22–25	[102]
LM25/10 wt%WC	10–50	500–2500	–	1.5–3.5		–	–	SEM	30–38	24–27	[116]
7071Al/x wt% SiC_p	15–30	1000–5000	–	2–5		EN32	–	Macro	29–34	19–14	[136]
Al1010/x wt% SiC_p	24	–	0.5–3	8		EN 31	Empirical Model	Macro	31–45	23–27	[127]
A319/10 wt%SiC_p	10–40	1800	15	2		–	–	SEM	34–39	19–14	[122]
LM13/10 wt%TiS_2	20–40	600–1600	–	1.5–3.5		EN 32	Taguchi method	SEM, ANONA	23–31	12–17	[125]
A356/Mg_2Si	10–40	1200–3000	–	1.15		EN 32	–	SEM	23–26	–	[131]
A356/x wt% SiC_p	10–120	330	–	0.2–0.4		EN 31	–	SEM	32–37	–	[132]
Al/9 wt% Al_2O_3 + 3 wt% Gr	10–30	1500	–	1–3		EN 32	Taguchi method	SEM, ANONA	21–36	–	[134]
LM13/10 wt% B_4C	10–30	1300	–	2.4		EN 32	Taguchi method	SEM, ANONA	28–32	18–24	[135]
Al1010/x wt% SiC_p	14–44	–	1–4	8		EN 31	Empirical Model	Macro, ANONA	47–31	28–24	[139]
LM25/10 wt%AlB_2	33–80	–	5	15	Dry Abrasion Tester	–	–	SEM	24–28	15–18	[114]
LM25/10 wt%AlB_2	33–80	–	–	10–20		–	Taguchi method	SEM, ANONA	22–26	14–18	[115]
LM25/10 wt%Si_3N_4	33–80	–	7	10–20		–	–	SEM	37–46	28–33	[117]
Al–12Si–Cu alloy/10 wt% of B4C, SiC, Al_2O_3, TiB_2	28–80	–	3–9	5–20		–	–	SEM	24–33	–	[123]
Al–12Si–Cu alloy/10 wt% B_4C	28–52	–	5	10–20		–	Taguchi method	SEM, ANONA	15–25	7–18	[124]
LM25/10 wt%TiC	10–40	400–2000	–	0.5–3		EN32	R.M.S method	SEM, ANONA	44–37	–	[133]

4 Research Gaps and Future Directions

The demand of FGAMCs has been increased in the recent years produced through centrifugal casting process. The FGAMCs have attracted researchers and industry because of the integral characteristics of changing conventional composites, the reduction in conceivable materials and the save of costs related to the centrifugal casting process. In practice many advanced FGM processing methods, such as additive manufacture and chemical vapor deposition,

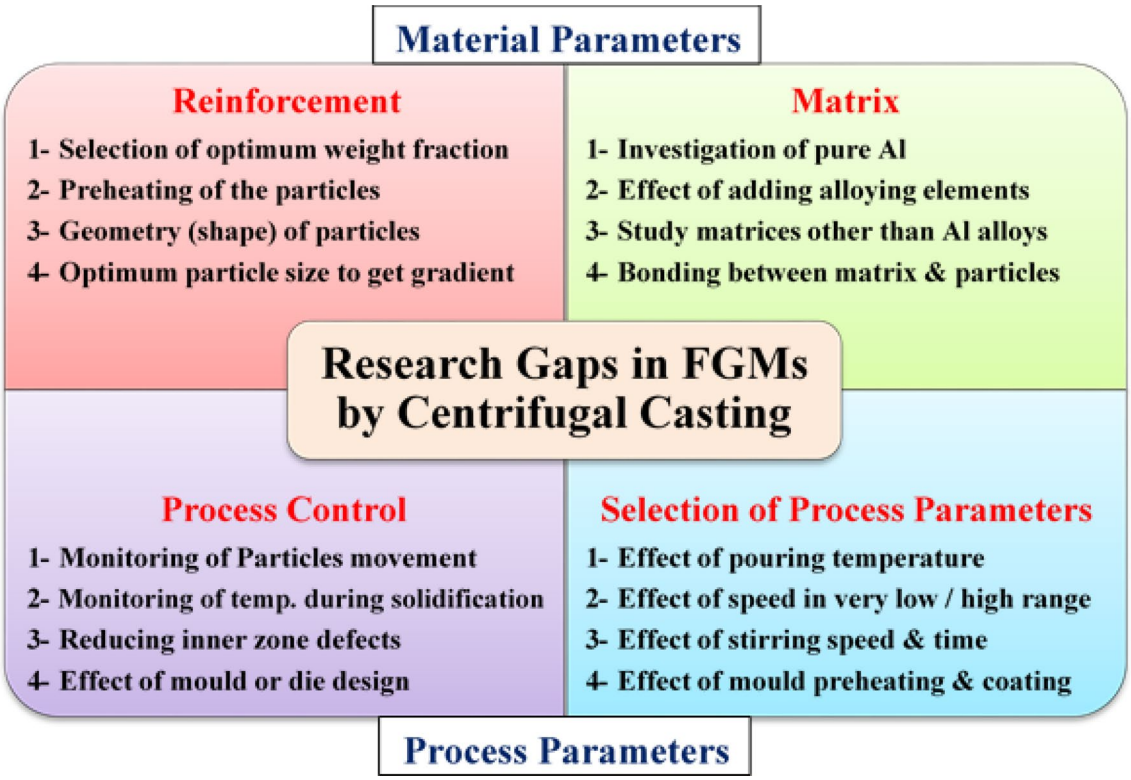

Fig. 39 Material and process parameters of research gaps for FGMs

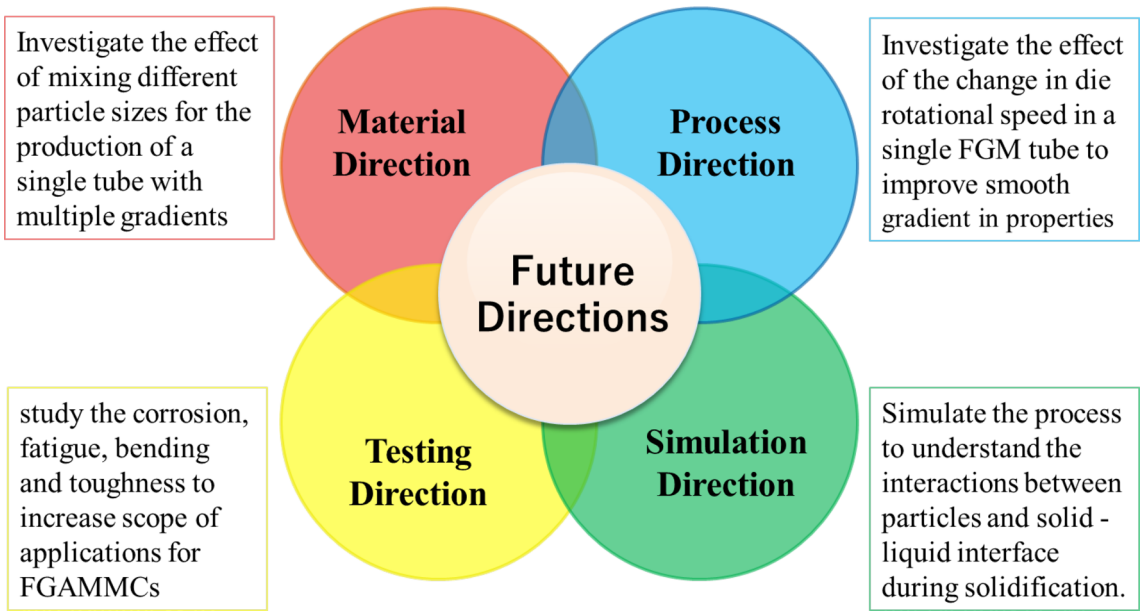

Fig. 40 Future directions for FGAMCs produced by centrifugal casting technique

have no control over gradient products, such as discrete structure, large-form production, tools and costs in comparison to centrifuge casting technique. Therefore, the two main inhibitors of FGM production using other methods are cost and technology.

There have been reports of research areas to produce FGAMCs manufactured through centrifugal casting processes. Research concluded by several researchers showed the improvement of the mechanical, tribological and microstructure behavior of FGAMCs.

The parameters effect on properties of the FGAMCs fabricated via centrifugal casting can be divided into two groups. The first group consists of process parameters such as rotation speed of the mould, pouring temperature, mould preheating temperature and mould coating, whereas the second group consists of material parameters such as reinforcement material (type, size, weight or volume, and shape) and matrix material [80]. The influence of material and process parameters on the microstructure, mechanical and tribological properties of FGAMCs were reported by various researchers, but many research issues remain to be studied as shown in Fig. 39.

On the other hand, future guidelines of FGAMCs fabricated through centrifugal casting technique are aimed mainly at improving mechanical and tribological characteristics and improving the quality of distribution of particles inside a matrix to achieve the best smooth gradient. Figure 40 shows the four directions of FGAMCs via Centrifugal casting process.

The process direction of research will expect control the centrifugal process itself through using variable mould rotational speed (and/or different cooling rates) of the single FG tube rather than the constant speed used in the previous works. The variable rotational speed and different cooling rates will give more control over distribution and gradient of particles and achieves a smoother gradient.

The material direction is expected to improve in gradient of the FG product by using more than one size of the same particles (double FGM), or by using a combination of two or more of the same size particles (hybrid FGMs) to achieve a smoother gradient. Therefore, the mechanical properties and wear resistance of FG products will be increase.

The third direction is to develop a 3-D numerical analysis or simulation of the solidification process under the effect of centrifugal forces. This model or simulation will help researchers to understand the interactions between particles and solid–liquid interface, thus improve gradient of particles. The final direction is to increase the scope of applications for FGAMCs manufactured through centrifugal casting by conducting tests such as corrosion, bending, toughness and fatigue under different loading conditions.

In fact, FGAMCs obtained through the centrifugal casting route are still a research area of interest to many researchers and therefore this research area is very active.

5 Summary and Concluding Remarks

This review paper focuses on the effect of reinforcement type and wear test parameters on the microstructure and wear properties of the FGAMCs fabricated through centrifugal casting route. FGAMCs are an exquisite class of graded materials that are designed and manufactured for special functional needs. One of the most versatile and economic methods of FGM production is centrifugal casting technology. The higher surface quality of FGM products by centrifugal casting technology, however, remained a distant dream compared to the other techniques.

FGMs have gained in prominence because of their diversifying applications in various fields such as aerospace, structural, automotive, power generation, microelectronics, bioengineering, etc. FGMs have good mechanical properties and wear resistance and even at high temperatures can retain their properties if design and process are correct.

An insight into the applications of FGAMCs suggests that the effort made in this area will be worthwhile because of the vastness of the FGAMCs produced through centrifugal casting applications such as hollow tubes, piping system, cylinder liners, pistons and diving cylinder. It is a known fact that with a single method it is impossible to process all materials successfully. From the conventional ways of centrifugal casting methods, the scientists and researchers tried out a lot of practical, more easy and economical ways of casting new materials for specific applications.

This review paper guides the new scientists into producing and characterizing FGAMCs wear properties reinforced with different types of reinforcement particles (like SiC, Al_2O_3, B_4C, WC, ZrO_2, Si_3N_4 and AlB_2) produced by centrifugal casting method.

This current review showed that the microstructure, mechanical characteristics and the wear resistance in the external zone or internal zone are better and depend on the distribution of the particles used compared with the matrix alloy. Moreover, the particle size (i.e. the particle density) significantly changes the gradient of the FG material in the base alloy, followed by the weight fraction (wt%) of particles. Furthermore, the applied load has also had a significant influence on the wear rate, which is followed by sliding distance, sliding speed and other wear test parameters, as indicated in the previous results.

Acknowledgements The study was supported by the National Natural Science Foundation of China (Grant No. 51979099),the

Natural Science Foundation of Jiangsu Province of China (Grant No. BK20191303), the Fundamental Research Funds for the Central Universities (Grant No. 2018B48414 and 2019B79814), Postgraduate Education Reform Project of Jiangsu Province (JGLX19_027), The Key Research and Development Project of Jiangsu Province of China (Grant No.BE2017148).

Compliance with ethical standards

Conflict of interest The author declares that they have no conflict of interest.

References

1. S. Maimunnisa, P. Gore, T.P.D. Rajan, V.S. Raja, J. Mater. Eng. Perform. (2018). https://doi.org/10.1007/s11665-018-3508-2
2. L. Ceschini, R. Montanari, *Advances in Metal Matrix Composites* (Trans Tech Publications Ltd, Zürich, 2011)
3. T.P.D. Rajan, J. Mater. Sci. **3**, 3491 (1998)
4. P.K. Gupta, R.K. Srivastava, Mater. Today Proc. **5**, 18761 (2018). https://doi.org/10.1016/J.MATPR.2018.06.223
5. J.Y. Fakruddinali, K.S. Badarinarayan, Ind. J. Sci. Res. Technol. **3**, 34 (2015)
6. Y. Miyamoto, *Functionally Graded Materials: Design, Processing and Applications* (Kluwer Academic, Dordrecht, 1999)
7. N.B. Duque, Z.H. Melgarejo, O.M. Suarez, Mater. Charact. **55**, 167 (2005)
8. R.M. Mahamood, E.T. Akinlabi, JMADE **84**, 402 (2015)
9. Himasekhar Sai, Int. J. Curr. Eng. Technol. **8**, 79 (2018)
10. A. Mortensen, S. Suresh, J. Int. Mater. Rev. **40**, 239 (1995). https://doi.org/10.1179/imr.1995.40.6.239
11. J.J. Sobczak, L. Drenchev, J. Mater. Sci. Technol. **29**, 297 (2013)
12. M. Koizumi, Compos. B **28B**, 1 (1997)
13. F. Ebrahimi, *Advances in Functionally Graded Materials and Structures*. (INTECH Open, Croatia, 2016)
14. D.K. Jha, T. Kant, R.K. Singh, Compos. Struct. **96**, 833 (2013)
15. V. Bhavar, P. Kattire, S. Thakare, S. Patil, R.K.P. Singh, IOP Conf. Ser. Mater. Sci. Eng. (2017). https://doi.org/10.1088/1757-899X/229/1/012021
16. Y. Miyamoto, Mater. Technol. **11**, 230 (1996)
17. D. Mahmoud, M. Elbestawi, J. Manuf. Mater. Process. **1**, 13 (2017)
18. R.S. Parihar, S.G. Setti, R.K. Sahu, Sci. Eng. Compos. Mater. (2016). https://doi.org/10.1515/secm-2015-0395
19. A. Shapiro, Z. Liu, A.M. Beese, Acta Mater. (2016). https://doi.org/10.1016/j.actamat.2016.12.070
20. I.M. El-Galy, B.I. Saleh, M.H. Ahmed, SN Appl. Sci. (2019). https://doi.org/10.1007/s42452-019-1413-4
21. J. Zhu, Z. Lai, Z. Yin, J. Jeon, S. Lee, Mater. Chem. Phys. **68**, 130 (2001)
22. Y. Watanabe, O. Inaguma, H. Sato, E. Miura-Fujiwara, Materials (Basel) **2**, 2510 (2009)
23. A. Arenas, L.A. Rocha, A. Velhinho, Materials (Basel). **7**, 8151 (2014)
24. A. Strojny et al., J. Mater. Eng. Perform. **25**, 3173 (2016)
25. D. Kim, K. Park, K. Kim, T. Miyazaki, S. Joo, H. Kwon, Mater. Sci. Eng. A (2018). https://doi.org/10.1016/j.msea.2018.12.128
26. E.I. Salama, S.S. Morad, A.M.K. Esawi, Materialia **7**, 100351 (2019)
27. A.K. Chaubey, R. Gupta, R. Kumar, B. Verma, S. Kanpara, S. Bathula, S.S. Khirwadkar, A. Dhar, Fusion Eng. Des. **135**, 24 (2018)
28. Z.H. Melgarejo, O.M. Suárez, K. Sridharan, Compos. A **39**, 1150 (2008)
29. Z. Yan-bo, L.I.U. Chang-ming, W. Kai, Z.O.U. Mao-hua, X.I.E. Yong, Trans. Nonferrous Met. Soc. China **20**, 361 (2010)
30. Y. Watanabe, H. Sato, in *Nanocomposites with Unique Properties and Applications in Medicine and Industry*, chap. 7, ed. by J. Cuppoletti (InTech, Rijeka, Shanghai and New York, 2011), pp. 133–150
31. Y.M. Lim, Y.J. Park, Y.H. Yun, K.S. Hwang, Ceram. Int. **28**, 37 (2002)
32. G.F. Yin et al., Thin Solid Films **345**, 67 (1999)
33. C. Deng, H. Kim, H. Ki, Compos. B (2019). https://doi.org/10.1016/j.compositesb.2018.12.101
34. C. Zhang, F. Chen, Z. Huang, M. Jia, G. Chen, Y. Ye, Y. Lin, W. Liu, B. Chen, Q. Shen, L. Zhang, E.J. Lavernia, Mater. Sci. Eng. A (2019). https://doi.org/10.1016/j.msea.2019.138209
35. D. Herzog, V. Seyda, E. Wycisk, C. Emmelmann, Acta Mater. **117**, 371 (2016). https://doi.org/10.1016/j.actamat.2016.07.019
36. M. Bodaghi, A.R. Damanpack, W.H. Liao, Mater. Des. **135**, 26 (2017)
37. D.W. Hutmacher, M. Sittinger, M.V. Risbud, Trends Biotechnol. **22**, 354 (2004)
38. K. Feng, H. Chen, J. Xiong, Z. Guo, Mater. Des. **46**, 622 (2013)
39. J. Zygmuntowicz, M. Wachowski, P. Piotrkiewicz, A. Miazga, W. Kaszuwara, K. Konopka, Compos. B **173**, 106999 (2019)
40. B.S. Shariat, Q. Meng, A.S. Mahmud, Z. Wu, R. Bakhtiari, J. Zhang, F. Motazedian, H. Yang, G. Rio, T. Nam, Y. Liu, Mater. Des. **124**, 225 (2017)
41. B. Kieback, A. Neubrand, H. Riedel, Mater. Sci. Eng. A **362**, 81 (2003)
42. B.C. Pai, T.P.D. Rajan, IJAEA **2**, 64 (2009)
43. K. Shah, A. Khan, S. Ali, M. Khan, A.J. Pinkerton, Mater. Des. **54**, 531 (2014)
44. G. Udupa, S.S. Rao, K.V. Gangadharan, Procedia Mater. Sci. **5**, 1291 (2014)
45. D.T. Sarathchandra, S.K. Subbu, N. Venkaiah, Mater. Today Proc. **5**, 21328 (2018)
46. P. Muller, J.-Y. Hascoet, P. Mognol, Rapid Prototyp. J. **20**, 511 (2014)
47. W. Meng, W. Zhang, W. Zhang, X. Yin, L. Guo, B. Cui. Int. J. Adv. Manuf. Technol. (2019). https://doi.org/10.1007/s00170-019-04061-x
48. S. Karnati, Y. Zhang, F.F. Liou, J.W. Newkirk, Metals (Basel). **9**, 287 (2019). https://doi.org/10.3390/met9030287
49. G. Marinelli, F. Martina, H. Lewtas, D. Hancock, S. Ganguly, S. Williams, G. Marinelli, F. Martina, H. Lewtas, D. Hancock, Sci. Technol. Weld. Join. (2019). https://doi.org/10.1080/13621718.2019.1586162
50. F. Erdemir, A. Canakci, T. Varol, Trans. Nonferrous Met. Soc. **25**, 3569 (2015)
51. T. Kunimine, H. Sato, E. Miura-Fujiwara, Y. Watanabe, in *Chap. 2 New Processing Routes for Functionally Graded Materials and Structures through a Combination of Powder Metallurgy and Casting, Advances in Functionally Graded Materials and Structures*, ed. by F. Ebrahimi (InTech - Open, Rijeka, 2016), pp. 33–48. ISBN 978-953-51-2274-6
52. X. Huang, C. Liu, J. Mater. Process. Technol. **211**, 1540 (2011)
53. K. Gupta, H. Saini, M.A. Zaidi, J. Mater. Sci. Mech. Eng. **4**, 163 (2017)
54. E.D. Eidel'man, M.A. Durnev, Tech. Phys. **63**, 1615 (2018)
55. X. Lin, C. Liu, H. Xiao, Compos. B **45**, 8 (2013)
56. M.R. Rahimipour, M. Sobhani, Metall. Mater. Trans. B **44**, 1120 (2013). https://doi.org/10.1007/s11663-013-9903-z
57. M. Naebe, K. Shirvanimoghaddam, Appl. Mater. Today **5**, 223 (2016)
58. G. Chirita, D. Soares, F.S. Silva, Mater. Des. **29**, 20 (2008)
59. E. Müller, Č. Drašar, J. Schilz, W.A. Kaysser, Mater. Sci. Eng. A **362**, 17 (2003)

60. E.S.C. Chin, Mater. Sci. Eng. A **259**(259), 155 (1999)
61. Y. Li, S. Jian, Z. Min, Key Eng. Mater. **280–283**, 1925 (2005)
62. W. Pompe, H. Worch, M. Epple, W. Friess, M. Gelinsky, P. Greil, U. Hempel, D. Scharnweber, K. Schulte, Mater. Sci. Eng. A **362**, 40 (2003)
63. S. Tharaknath, R. Ramkumar, B. Lokesh, Middle-East J. Sci. Res. **24**, 124 (2016)
64. I. Bharti, N. Gupta, K.M. Gupta, Int. J. Mater. Mech. Manuf. **1**, 221 (2013)
65. M. Wośko, B. Paszkiewicz, T. Piasecki, A. Szyszka, R. Paszkiewicz, M. Tłaczała, Opt. Appl. **35**, 663 (2005)
66. R.M. Mahamood, E.T. Akinlabi, M. Shukla, S. Pityana, in: *World Congress on Engineering 2012*, vol. III (2012)
67. G. Udupa, S. Shrikantha Rao, K.V. Gangadharan, in *Proceedings of the International Conference on Advances in Engineering, Science and Management* (Nagapattinam, 2012), p. 399
68. A. Gupta, M. Talha, Prog. Aerosp. Sci. **79**, 1 (2015)
69. J.W. Gao, C.Y. Wang, Mater. Sci. Eng. A **292**, 207 (2000)
70. E.J. Babu, T.P.D. Rajan, S. Savithri, U.T.S. Pillai, B.C. Pai, Theoretical analysis and computer simulation of the particle gradient distribution in a centrifugally cast functionally gradient material. Paper presented at the international symposium of research students on materials science and engineering, Chennai, 2004
71. P. Abdulsamad, K. Sandeep, P.R. Shalij, Int. J. Innov. Res. Sci. Eng. Technol. An **3**, 14441 (2014)
72. T. Ogawa, Y. Watanabe, H. Sato, I. Kim, Y. Fukui, Compos. A **37**, 2194 (2006)
73. H. Thai, S. Kim, *A Review of Theories for the Modeling and Analysis of Functionally Graded Plates and Shells* (Elsevier, Amsterdam, 2015). https://doi.org/10.1016/j.compstruct.2015.03.010
74. L.L. Mishnaevsky Jr., Compos. Sci. Technol. **66**, 1873 (2006)
75. N. Stein, J. Felger, W. Becker, Int. J. Adhes. Adhes. (2017). https://doi.org/10.1016/j.ijadhadh.2017.02.001
76. D. Almasi, M. Sadeghi, W.J. Lau, F. Roozbahani, N. Iqbal, Mater. Sci. Eng. C **64**, 102 (2016)
77. Z.H. Melgarejo, O.M. Sua, Scr. Mater. **55**, 95 (2006)
78. S.C. Ferreira, L.A. Rocha, E. Ariza, P.D. Sequeira, Y. Watanabe, J.C.S. Fernandes, Corros. Sci. **53**, 2058 (2011)
79. T.P.D. Rajan, B.C. Pai, Trans. Indian Inst. Met. **62**, 383 (2009)
80. B. Saleh, J. Jiang, A. Ma, D. Song, D. Yang, Met. Mater. Int. (2019). https://doi.org/10.1007/s12540-019-00273-8
81. S.D.S. Sunilraj, G.R.S. Ravishankar, Trans. Indian Inst. Met. **69**, 699 (2016)
82. L.S. Rao, K.R.A.K. Jha, Trans. Indian Inst. Met. (2018). https://doi.org/10.1007/s12666-018-1276-1
83. B.C. Pai, T.P.D. Rajan, Acta Met. Sin. (Engl. Lett.) **27**, 825 (2014)
84. X.H. Qin, W.X. Han, C.G. Fan, J. Mater. Sci. Lett. **21**, 665 (2002)
85. D.H. Song, Y.H. Park, Y.H. Park, I.M. Park, K.M. Cho, Mater. Sci. Forum **536**, 1565 (2007)
86. T.P.D. Rajan, R.M. Pillai, B.C. Pai, Int. J. Cast Met. Res. **21**, 214 (2008)
87. T.P.D. Rajan, E. Jayakumar, B.C. Pai, Trans. Indian Inst. Met. **65**, 531 (2012)
88. K. Wang, J. Cheng, W. Sun, H. Xue, J. Compos. Mater. **46**, 1021 (2011)
89. T.P.D. Rajan, R.M. Pillai, B.C. Pai, Mater. Charact. **61**, 923 (2010)
90. A.C. Vieira, P.D. Sequeira, J.R. Gomes, L.A. Rocha, Wear **267**, 585 (2009)
91. K.V. Babu, J.W. Jappes, T. Rajan, M. Uthayakumar, Proc. Inst. Mech. Eng. L J. Mater. Des. Appl. **230**, 182 (2016)
92. R. Rodrıguez-Castro, R.C. Wetherhold, M.H. Kelestemur, Mater. Sci. Eng. A **323**, 445 (2002)
93. S.R. Vikas, U.M. Maiya, E. Jayakumar, T.P.D. Rajan, B.C. Pai, Nagaraja, Int. J. Adv. Mech. Robot. Eng. **1**, 61 (2014)
94. Ö. Savaş et al., Sci. Eng. Compos. Mater (2014). https://doi.org/10.1515/secm-2014-0141
95. E. Jayakumar, A.P. Praveen, T.P.D. Rajan, B.C. Pai, Trans. Indian Inst. Met. (2018). https://doi.org/10.1007/s12666-018-1442-5
96. M. Sam, N. Radhika, Part. Sci. Technol. (2017). https://doi.org/10.1080/02726351.2017.1364312
97. S.C. Ferreira, A. Velhinho, L.A. Rocha, F.M.B. Fernandes, Mater. Sci. Forum **588**, 207 (2008)
98. A. Velhinho, Int. J. Mater. Prod. Technol. (2010). https://doi.org/10.1504/IJMPT.2010.034265
99. V. Bharath, S.S. Ajawan, M. Nagaral, V. Auradi, S.A. Kori, J. Inst. Eng. Ser. C (2018). https://doi.org/10.1007/s40032-018-0442-x
100. T. Prasad, N. Chikkanna, Int. J. Adv. Eng. Technol. **II**, 161 (2011)
101. S. Junus, A. Zulfia, Mater. Sci. Forum **857**, 179 (2016)
102. B.I. Saleh, M.H. Ahmed, Met. Mater. Int. (2019). https://doi.org/10.1007/s12540-019-00391-3
103. U. Pandey, R. Purohit, P. Agarwal, S.K. Dhakad, R.S. Rana, Mater. Today Proc. **4**, 5452 (2017)
104. R. Jojith, N. Radhika, U. Vipin, Trans. Indian Inst. Met. (2018). https://doi.org/10.1007/s12666-018-1523-5
105. N. Radhika, R. Raghu, Mat. Wiss. U. Werkstofftech **48**, 882 (2017)
106. K.R. Ramkumar, S. Sivasankaran, F.A. Al-mufadi, S. Siddharth, Arch. Civ. Mech. Eng. **19**, 428 (2019)
107. R. Singh, R.N. Rai, AIP Conf. Proc. **1943**, 020073 (2018). https://doi.org/10.1063/1.5029649
108. A.G. Rao, M. Mohape, V.A. Katkar, D.S. Gowtam, V.P. Deshmukh, A.K. Shah, Mater. Manuf. Process. **25**, 37 (2010)
109. N. Radhika, R. Raghu, J. Tribol. **137**, 1 (2015)
110. H. Abdizadeh, M. Baghchesara, Mech. Compos. Mater. **49**, 571 (2013)
111. N. Radhika, R. Raghu, Int. J. Mater. Res. **106**, 1 (2015)
112. N. Radhika, Iran. J. Mater. Sci. Technol. **13**, 41 (2016)
113. R. Jojith, N. Radhika, Mater. Res. Express (2019). https://doi.org/10.1088/2053-1591/ab1039
114. N. Radhika, R. Raghu, Tribol. Online **3**, 487 (2016)
115. N. Radhika, R. Raghu, Part. Sci. Technol. (2016). https://doi.org/10.1080/02726351.2016.1184728
116. R. Jojith, N. Radhika, J. Braz. Soc. Mech. Sci. Eng. **40**, 1 (2018)
117. N. Radhika, Sci. Eng. Compos. Mater (2016). https://doi.org/10.1515/secm-2015-0160
118. A. Kumar, G.D. Thakre, P.K. Arya, A.K. Jain, Ind. Eng. Chem. Res. **56**, 3527 (2017)
119. V.V. Monikandan, M.A. Joseph, P.K. Rajendrakumar, Resour. Technol. (2016). https://doi.org/10.1016/j.reffit.2016.10.002
120. M.S. Prabhudev, V. Auradi, K. Venkateswarlu, N.H. Siddalingswamy, S.A. Kori, Procedia Eng. **97**, 1361 (2014)
121. M.S. Surya, G. Prasanthi, Tribol. Ind. **40**, 247 (2018). https://doi.org/10.24874/ti.2018.40.02.08
122. D.E. Jayakumar, J.C. Jacob, T.P.D. Rajan, M.A. Joseph, B.C. Pai, Mater. Sci. Forum **831**, 456 (2015)
123. N. Radhika, R. Raghu, Trans. Nonferrous Met. Soc. China **26**, 905 (2016)
124. N. Radhika, R. Raghu, Procedia Eng. **97**, 713 (2014)
125. N. Radhika, Tribol. Ind. **38**, 425 (2016)
126. N. Radhika, R. Raghu, J. Eng. Sci. Technol. **12**, 1386 (2017)
127. I.M. El-Galy, M.H. Ahmed, B.I. Bassiouny, Alexandria Eng. J. **56**, 371 (2017)
128. P. Taylor, B.S. Yigezu, P.K. Jha, M.M. Mahapatra, Tribol. Trans. **56**, 546 (2013)
129. R.C. Cozza, Integr. Med. Res. **4**, 144 (2018)
130. J.G. Alotaibi, B.F. Yousif, T.F. Yusaf, J. Eng, Tribol. **0**, 1 (2014)
131. S.C. Ram, K. Chattopadhyay, I. Chakrabarty, *Mater. Res. Express* **5** (2018)

132. A.S. Karun, T.P.D. Rajan, U.T.S. Pillai, B.C. Pai, J. Compos. Mater. (2015). https://doi.org/10.1177/0021998315602946
133. N. Radhika, R. Raghu, Part. Sci. Technol. (2016). https://doi.org/10.1080/02726351.2016.1223773
134. N. Radhika, A. Vaishnavi, G.K. Chandran, Tribol. Ind. **36**, 188 (2014)
135. L.V.P. Muddamsetty, N. Radhika, Tribol. Ind. **38**, 108 (2016)
136. T.R. Prabhu, Arch. Civ. Mech. Eng. **17**, 20 (2017)
137. A. Ulukoy, M. Topcu, S. Tasgetiren **230**, 143 (2016)
138. A.G. Arsha, E. Jayakumar, T.P.D. Rajan, V. Antony, B.C. Pai, *Mater. Des.* **88** (2015)
139. I.M. El-Galy, B.I. Bassiouny, M.H. Ahmed, Key Eng. Mater. **786**, 276 (2018)